LINKING PHOTOCHEMICAL CARBON TRANSFORMATIONS AND MICROBIAL RESPONSES IN THE AMAZON RIVER PLUME

by

JOANNA LOUISE GREEN

(Under the Direction of William L. Miller)

ABSTRACT

This work focuses on the interplay between sunlight-driven and microbe-driven transformation of dissolved organic matter (DOM) from a dynamic system, the Amazon River plume. To mimic the mixing of river water with the ocean, organic matter was collected from river and low-salinity plume water, filter-sterilized, irradiated, and then inoculated with microbial communities from down-plume along the salinity gradient. Bacterial production and respiration were measured by ^{3}H-leucine incorporation and oxygen consumption rates. The DOM was characterized spectrally via excitation-emission matrix fluorescence (EEMs) and analyzed with parallel factor (PARAFAC) analysis; generating three unique components that aligned with previous studies. Those identified as terrestrial in origin diminished with irradiation. Additions of low-salinity organic matter stimulate bacterial activity in the saltier plume, sub-plume, and oceanic water. Short-term solar exposure to this organic matter enhances the stimulatory effect further. The DOM starting material and the microbial community selected determine the rates of the carbon transformations.

INDEX WORDS: Photochemistry; Environmental Microbiology; Amazon River; River Plume; Dissolved Organic Matter, PARAFAC; Excitation-Emission Matrix; Fluorescence

LINKING PHOTOCHEMICAL CARBON TRANSFORMATIONS AND MICROBIAL RESPONSES IN THE AMAZON RIVER PLUME

by

JOANNA LOUISE GREEN

Bachelors of Science, Georgia Institute of Technology, 2006

A Thesis Submitted to the Graduate Faculty of The University of Georgia in Partial Fulfillment of the Requirements for the Degree

MASTER OF SCEINCE

ATHENS, GEORGIA

2013

LINKING PHOTOCHEMICAL CARBON TRANSFORMATIONS AND MICROBIAL RESPONSES IN THE AMAZON RIVER PLUME

by

JOANNA LOUISE GREEN

Major Professor: William L. Miller

Committee: Patricia Yager
Mary Ann Moran

Electronic Version Approved:

Maureen Grasso
Dean of the Graduate School
The University of Georgia
May 2013

ACKNOWLEDGEMENTS

This work was supported by the National Science Foundation and the Gordon and Betty Moore Foundation. I'd like to thank the Captain and crew of the R/V *Melville* and R/V *Atlantis*. A big "thank you" to all of the ANACONDAS & ROCA Team members, the best group I've ever been to sea with. I can't wait to see what you guys do next and hope we all stay in touch.

First, thank you to my advisor, Bill Miller and the Miller lab for allowing a "bug" person into the lab and for all the hours of assistance learning photochemistry. I always knew Bill was on my side and would help me find my way. His jovial attitude prevented many a breakdown.

To Tish Yager, for allowing me the opportunity to join in her Amazon research and my thesis to be a part of such an amazing project. For being direct, even when it increased my doubts, I really do appreciate the honesty. The Yager lab members also deserve my appreciation. For folding me into the group and re-inspiring me, when to my eyes, my thesis has lost its shine.

And to Mary Ann Moran, who was always the quickest to respond to any of my problems, even though she is continually busy. With even the first edits of my thesis I could see how much she improved the quality of my work. She is constantly an inspiration.

I also must thank Annette Hynes, who had no stake in my project, but helped me anyways. From data assistance to a shoulder to cry on, I could always count on her. Shimmies!

To Randy Fulweber for assistance with maps and more importantly, for supporting me emotionally, although he was on the other side of the continent. I'd be even crazier without you.

Last, but far from least, I must give a big thank you to my family for their love and support. From sending cards and packages, to just listening to me; I appreciate all you've done.

TABLE OF CONTENTS

LIST OF TABLES

Page

LIST OF FIGURES

Page

CHAPTER 1

INTRODUCTION

Rivers are the main aquatic connection between land and the ocean, and serve as one of the largest influences on the marine carbon cycle. When a river mixes into the ocean, the resulting dynamics on the ecosystem are complicated, especially when considering large rivers (Gattuso et al. 1998, Wollast 1998). In terms of output, there is no larger river than the Amazon River, with an average discharge of 1.8×10^5 m^3 s^{-1} and a total carbon flux of 0.031 Pg C y^{-1} (Oltman 1968, Richey et al. 1991). The location of the Amazon River mouth near the equator also creates unique mixing interactions with weak Coriolis forces causing a minimally retroflected plume, thus delivering riverine material great distances zonally into the Atlantic Ocean. A detailed description of the riverine plume effects and dynamics are presented in Appendix H.

Discharge of all global riverine dissolved organic carbon (DOC) is sufficient to account for the entire pool of organic carbon dissolved in seawater, but only a small fraction of the organic matter found in marine systems appears to be land-derived (Hedges et al. 1997, Wollast 1998, Mackenzie et al. 2011, Massicotte and Frenette 2011). The mechanisms by which these substantial inputs of terrestrial matter might be destroyed are largely unknown. However photochemical processing has been indicated as an often over-looked component (Miller and Zepp 1995, Hedges et al. 1997, Bauer and Bianchi 2011).

Hedges and colleagues (1992) report the necessity for further study of "photolysis" in the Amazon River to explain the decrease of humic substances that cannot accounted for by microbial breakdown as it is delivered to the ocean (Hedges et al. 1992). The tropics in particular receive large amounts of solar radiation, thus increasing the potential for photochemical processing of organic material in the Amazon Plume (Zafiriou 1977, Geyer et al. 1991, Limeburner et al. 1995, Amon and Benner 1996a). The high levels of DOM and low salinity water that are delivered to the tropical Atlantic represent a vastly different water type than is typically found at its destination, which contains deep mixed layers with low DOM and high salinity (Del Vecchio and Subramaniam 2004, Cooley and Yager 2006).

The photochemical transformation of complex DOM can also create labile compounds that stimulate growth in the heterotrophic microbial community (Miller and Moran 1997, Kieber 2000). However, previous investigations of the interplay between marine photochemical reactions and microbial processes, what I will refer to here as photochemical/microbial linkage (PCML) studies, have a wide range of results in aquatic systems, with little consensus about microbial responses to irradiated organic material. The existing literature also has been dominated by limnological studies. For example, in a humic lake, researchers calculated an increase in bacterial biomass of up to 400% relative to dark controls after the addition of an 8 hour irradiated water sample (Bertilsson and Tranvik 1998). Conversely, working in a humic-rich brook, irradiated water samples lead to a 90% decrease in cell abundances as compared to the addition of a non-irradiated sample (Gjessing and Källqvist 1991). Of the 61 studies reviewed by Mopper and Kieber (2002), 40 showed stimulating microbial responses to pre-irradiated water (up to 580%) and 21 showed either adverse effects (less than 90%) or no

response (Mopper and Kieber 2002). Much of this variation could result from unique DOC characteristics for each location or from differences in experimental methodology. Part of the contradictions found within the literature may be due to which specific microbial community was selected to quantify DOM lability, particularly in light of the extensive evidence of spatial diversity inherent in microbial communities (DeLong 2009, Rodriguez-Brito et al. 2010). It seems important to choose a biologically-relevant indicator community that represents the population that will most likely encounter the irradiated DOC pool in the natural system being assessed.

The majority of aquatic environmental PCML studies involve freshwater lakes, small rivers, lagoons or other relatively stable systems. Many studies re-introduce irradiated water back to the resident community from where it was collected, which may be appropriate for these fairly static locations. For example, Abboudi et al. (2008) worked in a coastal bay without riverine input, a lagoon with two minor rivers, and an open coastal site. In these cases, it might be reasonable to assume that the resident community did not change significantly over the seven-hour irradiation. Piccini et al. (2009) used a similar method, employing a biolability indicator community isolated from the same source lagoon to evaluate changes in DOM pre-irradiated for six days.

Assuming the local bacterial community to be the best indicator of lability seems less justified, however, when evaluating the Amazon River or its plume, which exhibit high discharge rates (Oltman 1968, Muller-Karger et al. 1995). There are few PCML studies in dynamic, large river systems like the Amazon River Plume. Some research has been conducted with irradiated riverine DOM and a downstream marine microbial community, focusing primarily on the

availability of various DOM size classes (low molecular weight and high molecular weight) (Rochelle-Newall et al. 2004). That study, however, was carried out in a fjord in Denmark with low microbial diversity and low temperatures, and results may not be comparable to an tropical region where microbial diversity and metabolism rates are higher (Pommier et al. 2006, Fuhrman et al. 2008). The majority of work done in dynamic systems such as the Mississippi and Congo rivers, focuses primarily on specific molecular indicators like lignin, and not on the total DOM pool (Benner and Opsahl 2001, Spencer et al. 2010). These studies preferentially investigate the chemical processing and downplay the microbial aspect, although Benner and Opsal (2001) do measure amino acid concentrations as a microbial activity proxy.

While some PCML research has been carried out in the fresh waters of the Amazon River, no work has been done to date that follows the dynamics in the plume as the riverine DOM comes into contact with marine communities, or on mechanisms that directly connect riverine DOM to oceanic microbial processing of organic matter (Amon and Benner 1996a, Remington et al. 2011). Photo-oxidation experiments performed upriver indicate that photochemical breakdown might not be important within the inland riverine systems, a result suggested by the very small contribution of photochemical processes (0.05%) to CO_2 outgassing rates measured throughout the Amazonian basin (Remington et al. 2011). Much of this could be due to optical shading, both from arboreal canopy effects and self-shading due to suspended sediment. Thus microbial activity likely dominates the breakdown of organic matter within the river since the opportunity for photochemical processing is limited. This outcome would not be the case in a more UV-accessible region, for example, in the extended plume as it flows into the ocean, where it promotes mixing of riverine and marine waters. This mixing will dilute riverine DOM, as well

as initiate flocculation and deposition of large particles along the salinity gradient. Shading will occur less in a plume than in a river and UV radiation will be able to reach a greater proportion of macromolecules, thus increasing the importance of organic matter photolysis in these plume system (Del Vecchio and Subramaniam 2004, Cooley and Yager 2006, Abboudi et al. 2008).

To mimic these dynamic mixing processes in the plume, we collected riverine DOM source water from near the mouth of the river or in a low salinity plume location and mixed these irradiated waters with a down-plume or oceanic microbial community. Here, the more marine community represented a biolability indicator of the riverine organic matter before and after phototransformation. In this study, experiments were carried out by exposing each DOM source material to carefully quantified light doses to simulate the conditions for phototransformation of organic material in the surface plume as it is transported to and mixed with marine microbial communities. The significance of photochemical transformations within the DOM were measured using changes in optical properties, and responses of down-plume marine microbial activity were calculated from changes in microbial respiration and bacterial production rates (Ducklow 1992, Kirchman 2001, Labasque et al. 2004).

CHAPTER 2

METHODS

Field Sampling. Samples were collected from the Amazon River plume in September and October of 2011 on the R/V *Melville* and July 2012 on the R/V *Atlantis* using a CTD rosette, equipped with 10L Niskin bottles (Table 1). On each cruise, paired stations from dissimilar water types (one inner plume or riverine and one outer plume or oceanic) were selected on the basis of physical attributes such as salinity and organic matter concentrations. One of each pair was designated as the dissolved organic matter source (DOM source), in most cases characterized by low salinity and high colored dissolved organic material (CDOM). The other station of the pair was used as the source of the microbial community inoculum for the DOM lability bioassay. Natural source controls (unfiltered, un-mixed, non-irradiated) were collected from each site for comparison to experimental conditions. (Figure 1 & Table 1)

Sample Treatment. All water samples used in this study were gently gravity filtered (293 mm, 3-µm pore-size polycarbonate filter) to remove large detritus with minimal lysis of cellular material. The DOM source water was then filter sterilized through a 0.2-µm pore-size Whatman Polycap^{TM} 75AS capsule filter, with a subset of this filtrate checked for sterility using bacterial production and respiration measurements. DOM samples were stored in the dark after 0.2-µm filtration at 28-29°C for no more than 4 d before irradiation. The only exception was the aged DOM test, in which one low salinity plume sample (Station 6_2011) was aged by placing 3-µm filtered water in the dark at constant temperature of 28-29°C for one week to allow the *in situ*

heterotrophic microbial community to remove all biologically labile DOC prior to irradiations. In one experiment, a subset of the gravity filtered microbial community source water was filter sterilized through a 0.2-μm pore-size Whatman Polycap^{TM} 75AS capsule filter and then combined with the 3-μm filtrate from that same collection in order to test for dilution artifacts. All microbial community source samples were stored in the dark at 28-29°C until used for experiments within 4 h of collection (see Appendix A for sample processing diagram).

Irradiation Procedure. Approximately 1 L of the sterile DOM source filtrate was placed in a 1 L water jacketed glass beaker, with a Teflon® magnetic stir-bar, and glass stir rods added to prevent vortex-formation, covered with a quartz glass plate for 0, 6, or 12 h under a solar simulator (Suntest CPS, DSET Laboratories) equipped with a 1500 W xenon lamp (Heraeus) (Appendix B). The spectral irradiance was measured with an Olis 756 spectroradiometer, with an attached 60-cm fiber optic cable and a 2-inch integrating sphere. The spectroradiometer was calibrated with an OL 752-10 regulated power supply and a NIST standard tungsten halogen lamp. The total irradiation incident on the surface of the sample for the 6 and 12 h exposures were 1.61 x10^7 μmol photons per m^{-2} and 3.22 x10^7μmol photons per m^{-2}, respectively for a spectrum from 250 nm to 700 nm. For UV-radiation (280 nm – 400 nm) the photon dose was 1.5 x10^6 μmol photons per m^{-2} and 2.99 x10^6 μmol photons per m^{-2}. Comparing these UV dose values to modeled values over the same wavelength for clear sky at the equator during fall conditions (to compare to 2011 data) and summer conditions (to compare to 2012 data) (Leifer 1988), our 6 and 12 h exposures corresponded to 2.3 and 4.3 days of natural sunlight, respectively, for 2011 (fall) and 2.5 and 5 days for 2012 (summer).

Temperature was regulated at 28-29°C during irradiations and incubations with a Fisher Scientific® recirculating water bath and, in most cases, was within a degree of the *in situ* temperature of the source water (ranging from 27.74°C – 30.02°C) (Table 1). The various DOM samples were then combined in a 1:1 ratio with the 3-μm-filtered microbial source water. All mixtures were incubated in the dark pre-tritiated leucine addition for 24 h at 28-29°C as described for bacterial production measurements and 1 week for respiration measurements (Appendix A). This standard bacterial production incubation period was selected based on preliminary incubations designed to determine the minimum community response time when exposed to novel DOM as measured by leucine incorporation rates, using procedures described below (Appendix C). The 1-week respiration incubation was chosen to allow for complete processing of biologically labile DOM

Measurements of Bacterial Activity. Microbial production measurements were performed in triplicate (plus killed controls) using ^{3}H-leucine incorporation (Ducklow 1992, Smith and Azam 1992, Kirchman 2001). Samples from 2011 were run on a Beckman LS 6500 Liquid Scintillation Counter and samples from 2012 were run on a Perkin Elmer Tri-Carb Liquid Scintillation Counter, both machines were calibrated less than 3 months prior to usage and Ultima Gold™ was used as the scintillation cocktail in both cases. Production measurements were taken before and after incubation and the difference used to calculate relative responses for each sample.

For the 2011 cruise, total microbial respiration was quantified in triplicate following a week-long incubation with oxygen consumption data measured using a spectrophotometric Winkler method (Labasque et al. 2004). The 2012 cruise utilized triplicates incubations measured by a pulse-probe fluorescence oxygen probe (Ocean Optics, Foxxy Sensor) also incubated for 1 week to

quantify the amount of oxygen in each sample. The cross-calibration of the fluorescent probe with the Winkler measurements is detailed in Appendix D. Oxygen concentration was measured before and after 1-week incubations to determine respiration rates. For both methods of oxygen consumption, a respiratory quotient of 1 was used to calculate CO_2 production rates for bacterial carbon demand and growth rate efficiency and thus the metabolic ratio computations (Amon and Benner 1996b, Briand et al. 2004, Robinson and Williams 2005). A metabolic ratio was calculated using a formula similar to that of the bacterial growth rate efficiency using measured parameters and the formula below (del Giorgio and Cole 1998).

Bacterial Carbon Demand (BCD) = Bacterial Respiration + Bacterial Production

Bacterial Metabolic Ratio (BMR) = Bacterial Production / BCD

A range of respiration quotients were used to verify that the choice of RQ in the calculations could not completely account for observed variability. Values representing literature extremes were chosen for this analysis using 0.67 (saturated fatty acids) and 1.33 (glycolic acid) (Williams and del Giorgio 2005). This work is presented in Appendix E.

Optical Measurements and Analysis. All DOM source samples were analyzed optically to characterize the Fluorescent Dissolved Organic Matter (FDOM) with a Perkin Elmer Luminescence Spectrophotometer (model LS50B). Excitation Emission Matrix Spectra (EEMS) were determined using 5-nm excitation and emission bandwidths and an integration time of 0.25 seconds. Excitation and emission scans were recorded at 5-nm intervals over wavelength ranges of 250–500 nm and 280–700 nm respectively. EEMS were corrected for inner filter effects with measured CDOM spectra and for second-order Raman and Rayleigh scatter effects (Mobed et al. 1996) (McKnight et al. 2001) using Milli-Q water blanks. EEMS were converted to Raman units

(RU) using the area under the Milli-Q Raman scatter peak at an excitation of 350 nm. This calculation was done using the FLToolbox 1.91 created by Wade Sheldon (University of Georgia) for MATLAB® (Zepp et al. 2004).

Modeling of Optical Data and Analysis. PARAFAC analysis was performed as described in Stedmon and Markager (2005a). The EEMS input into the algorithm were run with 41 excitation wavelengths ×371 emissions wavelengths as detailed above. To assure adequate input levels our samples were supplemented with 6 samples from the same region collected by colleague Patricia Medeiros (University of Georgia) on the same 2012 cruise for a total of 30 samples. These samples include the 6 sterile-filtered DOM source waters with their respective irradiation times (0, 6, and 12 h, except for the riverine Station26_2012 which was subjected to an additional 18 and 24 h) totaling 20 DOM source samples, as well as sterile-filtered water from Station 9_2011 that was irradiated for 0, 6, and 12 h. EEMs were then combined into a 3-dimensional data array (30 samples × 41 excitation wavelengths × 317 emission wavelengths). This array was then analyzed by PARAFAC with the technique first described by Bro (1997). The PARAFAC modeling was carried out in MATLAB® (Mathworks, Natick, MA) with the DOM- Fluor toolbox and additional code written by Fang Cao (University of Georgia) (Murphy et al. 2008) (Yamashita et al. 2010).

Bacterial Abundances. Biological samples were fixed with 1% paraformaldehyde and stored at -80°C until counting. Each sample was stained with SYBR Green (Life Technologies) and mixed with Reference Beads (Spherotech, Fluorescent Yellow Particles, 1.7 - 2.2 um) (Gasol and Del Giorgio 2000) and run for 2 min in duplicate on a FACScalibur (BD) flow

cytometer. Standards were prepared using sterilized artificial seawater. Samples were analyzed using FlowJo software (Tree Star, Inc., Ashland, OR).

CHAPTER 3

RESULTS

Microbial Community Responses. All control experiments showed greater respiration and production values for the unfiltered, whole water DOM source samples than for its paired unfiltered, whole water microbial source sample, clearly indicating that the organic matter available in the inner plume was supporting more bacterial activity than that in the oceanic waters (Figure 11). The single exception, as expected, was the High Salinity 2 experiment in which a high salinity, low CDOM sample was used as the DOM source sample and was paired with a low salinity, high CDOM microbial source sample, which showed the opposite trends. The bacterial respiration rates and production rates, along with associated errors, are displayed in Table 2 and production values are shown in Figure 11. The bacterial metabolic ratio was the main parameter used to evaluate the microbial response, with respiration and production rates (Table 2) used secondarily to address unexpected BMR amounts, confirm trends, or check data quality.

The salinity of the DOM source water was used to categorize the experiments into three groups (Figure 1, Table 1). In the first group, a riverine DOM source (Stn10_2012) was combined with an oceanic microbial community (Stn15_2012). The respiration rates observed in these experiments (Table 2) are at the upper range of average rates observed in natural communities (from 0.4 – 23.3 mmol $O_2/m^3/d$), and in most cases were higher than expected compared to predictions using production rates (del Giorgio and Cole 1998, Robinson and Williams 2005).

Respiration rates of the high salinity microbial source sample provided with the riverine DOM source were three to eight times greater than production rates in the same pairing (Table 2).

The addition of the riverine DOM source water increased these low bacterial growth efficiencies in the microbial source water when compared to the un-manipulated microbial source water, by about 5%, with an additional increase after irradiation of up to 10% (Figure 2), although, the difference is not statistically significant. The riverine DOM stimulated marine microbial growth in all cases, but never quite reached the levels in terms of production, respiration or BMR of the native riverine community (Table 2) (Figure 2, 11).

In the second group of experiments, DOM in low salinity plume (LSP) water (Stn6_2011, Stn6_2011_Aged, or Stn11_2011) was irradiated and supplied to a microbial community source obtained from high salinity plume (HSP) water, with one experiment examining the response of a microbial community isolated from just below the plume (Stn13_2011(sub-plume community); Table 1). Microbial responses from LSP water showed various effects (Figure 3, 11), but in most cases, an increase in all microbial responses with irradiated LSP was apparent. In LSP 1 (Stn6_2011 to Stn9_2011), the whole water and filtered respiration rates were more than double the values for the production rates. After irradiation, both rates increase and became much closer with respiration only being approximately 100 nmol C/L/hr larger than production (Table 2) (Figure 3,11). In LSP 2, the low salinity plume sample (Stn6_2011) with the aged DOM, as discussed in the methods section, resulted in different trends from the un-aged sample from the same site. In non-irradiated treatments, the aged sample yielded lower production and respiration in the HSP communities than the non-aged samples from the same site before

irradiation. Trends were similar for all irradiation times except for values measured after 12 h of irradiation, which exhibited increased production rates at greater levels than the increase in respiration rates (over 200nmol C/L/h higher). There was an increase in all responses (production and respiration) due to irradiation regardless of whether or not the sample was aged (Table 2) (Figure 11). After 6 h irradiation, the BMR of the aged Stn6 was similar to that of the un-aged Stn6 sample. After 12 h of irradiation, the aged sample actually surpassed the non-aged sample, though not within significant levels (Figure 3). The LSP waters (Stn11_2011) inoculated with a sub-plume HSP community (Stn13_2011) yielded overall lower BMR values than the surface HSP microbial communities. This result was mostly driven by production values, as the respiration rates were fairly similar to the other LSP experiments (Table 2).

The third set of analyses used high salinity water (HS) as the DOM source material, either high salinity plume water or oceanic water. One experiment involved two side-by-side plume edge sites collected about 200 m apart across a front; one visibly in the plume and one visibly oceanic. In this case the high salinity plume water from Stn26Br_2011 was provided to the oceanic community collected from nearby Stn26Bl_2011 (Figure 1, Table 1). The oceanic microbes showed a lower production rate when mixed with the DOM from the plume when compared to unfiltered, untreated samples from either collection site. The respiration rate following mixing of the two, plume-edge samples was in between the respiration rates measured for the unfiltered source waters. Respiration jumped approximately 400 nmol C/L/hr and production rates surpassed respiration rates with values over 1,000 nmol C/L/hr (Table 2) (Figure 11). The plume edge site generates the largest increase in bacterial production response with irradiation relative to all experiments in this study. In the last pairing, which reversed the normal treatments

to test for artifacts of the method, high salinity coastal DOM (Stn5a_2012) was provided to a low salinity plume community (Stn6_2012). Respiration and production were reduced in the mixed, non-irradiated treatment as compared to the unamended community by approximately 100 nmol C/L/hr. This decrease was lessened with irradiation, but the increase was not as dramatic compared to other experiments. BMR values and production rates were lower in all cases when compared to community source water values from unfiltered, unmixed samples, although after 12 h of irradiation (Figure 4, 11), BMR and bacterial production rates increased with irradiation, but never exceeded values observed in untreated, whole water incubations.

Optics/EEMs/PARAFAC Analysis. The characterization of the FDOM with excitation emission matrices provides information on potential microbial metabolic substrates. These EEM diagrams are presented in Appendix F for the 24 samples utilized in the PARAFAC modeling, 21 of which were also used as DOM source samples, and 3 of which are additional samples from Stn9_2011. Duplicate EEMs from the unirradiated riverine sample, with the greatest potential for large complex terrestrial molecules (Stn10_2012), were included in the PARAFAC algorithm. These replicate EEMs from the same sample showed minimal differences, as displayed in Appendix G.

PARAFAC analysis of our 30 EEM runs yielded three unique components (C1, C2, C3; Figure 5, Appendix H). Comparable components have been defined previously in the literature from similar environments as shown in Table 4 (Coble 1996, Stedmon et al. 2003, Stedmon and Markager 2005, Murphy et al. 2008, Kowalczuk et al. 2009, Yamashita et al. 2010). The C1 FDOM component is consistent with a previously defined terrestrially-derived humic source and

is the most abundant component in all samples except for the high salinity sites (Stn26Br_2011 and Stn5a_2012) for which fluorescence values were at similar levels to those of C3. Among study sites, C1 was an order of magnitude more fluorescent in the riverine DOM (Stn10_2012) than in the low salinity plume stations (Stn6_2011 and Stn11_2011), which were in turn close to an order of magnitude larger than the high salinity stations (Stn26Br_2011 and Stn5a_2012).

All irradiations caused a decrease in measured C1 fluorescence over time, with loss rates higher in lower salinity samples. The percent contribution to the total fluorescence following irradiation (Figure 5) indicates a general lessening of excitation/emission in the FDOM region defined as Component 1 (C1), and increases in region C3. Throughout the irradiation, C1 decreases the most dramatically. Region C3 does not change substantially, but effects of irradiation are variable, showing a slight increase in the high salinity samples. The average F_{max} (the maximum fluorescence in a defined EEMs region) for C1 in the LSP sites dropped from 2.5 Ramen Units (RU) before irradiation to 1.9 RU after 12 h irradiation. The riverine sample showed the greatest absolute loss due to irradiation falling from an initial F_{max} of 10.7 RU to 8.1 RU after 12 h and 6.6 RU after 24 h. High salinity sites averaged an F_{max} of 0.4 RU prior to exposure and 0.2 RU after 12 h of irradiation (Figure 6).

The second component (C2) also is consistent with characteristics of terrestrial humics, having some descriptive overlap in the literature with C1 (Table 4) (Coble 1996, Stedmon et al. 2003, Stedmon and Markager 2005, Murphy et al. 2008, Kowalczuk et al. 2009, Yamashita et al. 2010). The riverine C2 (averge F_{max} = 1 RU) was more than 2.5 times larger than either the low (average F_{max} = 0.38 RU) or high salinity stations (average F_{max} = 0.21 RU), which were more

comparable to one another (Figure 7). C2 also generally decreased with increased irradiation dose, but not as significantly as was seen for C1. The higher salinity sites (including the LSP and HSP/Marine samples) are an exception to the general loss trend, showing a slight increase in the relative abundance of C2 after 6 h of irradiation, with a subsequent drop after 6 additional h of irradiation (12 h total). This trend was more pronounced with the aged DOM sample (Stn6_2011_Aged) and the plume edge site (Stn26Br_2011). The C2 fluorescence in the marine sample (Stn5a_2012) remained relatively constant at an Fmax of approximately 0.15 throughout the irradiation (Figure 7).

C3 is comparable to microbiological product peaks described in the literature, often noted specifically as organic compounds of algal origin, similar to tryptophan or polyphenol (Table 4) (Coble 1996, Stedmon et al. 2003, Stedmon and Markager 2005, Murphy et al. 2008, Kowalczuk et al. 2009, Yamashita et al. 2010). In the riverine station, C3 was about double that found in the other stations (non-irradiated F_{max} was almost 2 RU, where other F_{max} values were approximately 0.5 ±0.2 RU) (Figure 8). The aged DOM sample was the exception to this finding with C3 levels comparable to those found in the riverine station (Stn10_2012) (F_{max} across all riverine irradiation times was approximately 1.3 RU). The relative fluorescence of C3 did not change dramatically with irradiation except for the riverine site, which showed a decrease in C3 fluorescence with irradiation dose. The only other unique trend was observed in the plume edge, high salinity site (Stn26Br_2011), which had a similar trend to that found for C2 with an increase after the first irradiation time point followed by a loss during the second irradiation step (Figure 8).

Cell Abundance. The cell-count measurements conducted on the 3-µm filtered water samples indicated from 4 to 10% lower bacterial abundance than in the corresponding whole unfiltered sample. This effect of filtering on cell abundance was similar to what has been reported in the literature (Lemée et al. 2002, Reinthaler et al. 2005). Cell numbers did not change significantly during 24-h incubations with DOM, with the difference between groups being less than 1 standard deviation for each (Table 3). The 0.2-µm filtered samples showed 80±8% fewer cells than their whole water counterparts, with an average error of 8%, indicating that DOM samples were not entirely sterile, but cells were significantly reduced by the treatment. There was also an increase of 16 to 19% in cell abundance over the 24 h dark incubation in the controls. All the microbial source samples from the high salinity regions had similar cell counts to each other with an 8% within-group variation (Table 3).

Data supplied by ANACONDAS/ROCA project Collaborators:

Bacterial community structure. The bacterial community structure was determined using 454 pyrosequencing of the 16S ribosomal RNA subunit and supplied by Byron Crump (University of Maryland, personal communication). Results indicate high similarity of all high salinity plume and open ocean marine communities in the study region and strong similarity within the low salinity plume area. For most of our experiments, the biolability indicator community was selected from a high salinity region. This microbial community similarity does not hold true for experiments with the sub-plume community and HS2, which used a low salinity plume (LSP) community. The 16S rRNA data show that the sub-plume community and LSP communities are statistically different from those in the high salinity regions.

Estimated transit time from the Amazon River mouth to each sampling site. Values were calculated with a HYCOM model and supplied by Victoria Coles (University of Maryland, personal communication) based on tracking surface drifters in the plume region (Table 5). Model floats were released in a band parallel to the coastline, spanning from the region just to the north of the main Amazon channel to the south of the Tapajos Channel (2N, 50W to 0.5S, 48.5W). Floats were released in a randomized distribution with a width of 1-degree longitude. Floats that entered a square box 88km in width centered on a station location were considered to represent the age distribution of particles within the station location. Thus, even within the initialization region, water body age may be greater than zero if floats resided for more than a day in the region prior to moving out of the defined box. Model grid resolution is 19km, thus the choice of an 88km width region allows for integration of several grid cells into the computation. The model could not differentiate between the DOM source water station and the microbial community source station for HS1, involving the side-by-side plume edge stations Stn26_2011 (Br & Bl).

CHAPTER 4

DISCUSSION

In this study of the Amazon Plume region, riverine and low salinity DOM was found to stimulate the growth of marine and high salinity plume microbial communities, and in most cases photochemical processing of the DOM increased its lability, although not always at significant levels. Longer irradiations and/or incubations may be required to reproduce the full extent of the natural DOM processing that occurs within the plume. The estimated transit time for water calculated by Victoria Coles (University of Maryland) showed that our experiments could be viewed as under-irradiated compared to natural doses (Table 5). Since our longest irradiations of DOM prior to microbial incubations is estimated to represent about 5 days of natural sunlight, only the HS1 experiment might be considered over-irradiated as compared to natural photochemical processing

The microbial communities used as biolability indicators in this study are unlikely to be sufficiently different enough to account for observed variation in responses within each experimental grouping. The exceptions to this were experiments LS3 which used a sub-plume community, and HS2, which used a low salinity plume community. Consequently, results obtained in these two experiments using distinct community types might not be directly comparable when addressing the role of DOM lability from similar source material and exposure regimes.

Based on the choice of respiration quotients alone, and considering the range of literature values, the maximum possible variability of the BMR that could be ascribed to changes in substrate type is 20% (Appendix E). Respiration quotients for marine bacteria are rarely measured experimentally and an incorrect match between substrate and its corresponding quotient can lead to errors in interpretation of respiration measurements (Robinson and Williams 2005). This trend could be considered a plausible explanation for the apparent DOC lability changes documented here after specific irradiation time points. Use of saturated fatty acids (RQ= 0.67) by the microbial community results in greater observed ratio than for molecules like glycolic acid (RQ= 1.33). The latter are more complex in structure and potentially less sensitive to chemical alteration by UV radiation (Kieber 2000, Williams and del Giorgio 2005). Since most fatty acids are created biologically, in the sterile-filtered irradiations it is improbable that significant biological production occurred or that they were formed by random UV degradation of other organic molecules (Zhukova and Kharlamenko 1999, Nichols 2006). On the other hand, other photochemical studies have commonly found production of compounds comparable to glycolic acid and other short chain (unsaturated) fatty acids (Kieber and Mopper 1987, Münster 1993).

A recent study calculating RQ's with 72 direct measurements of RQ in 52 freshwater sites found that higher RQs were usually found in heterotrophic systems, with all values averaging approximately 1.2 (Berggren et al. 2011). Consequently, our assumed RQ of 1 might be an underestimate. While it is feasible that compounds more complex than the starting material could be created with irradiation, this is not likely. Most literature supports a decrease in MW as irradiation continues (Kieber and Mopper 1987, Frimmel 1994, Wetzel et al. 1995, Corin et al.

1996, Hernes and Benner 2003, Spencer et al. 2009). In any case, if a substrate change did occur during incubation (e.g. switching to smaller molecular weight products created by irradiation), this would most likely lead to a general lowering of BMR (Appendix E) which is not observed in our experiments (Figures 2 - 4).

There does appear to be a relationship between salinity and PARAFAC component abundance. The trends shown in Figure 5 indicate the terrestrial C1 is more sensitive to UV irradiation than the other components whose percent contributions stay relatively stable. The exception is the high salinity water experiments, which indicate a slight increase in C2. This relationship could be due to a variety of factors specific to individual components (see below). The ratio of terrestrial C1 to microbially-derived C3 follows salinity trends (Figure 9) when considering the salinity difference between the source of the microbial community (all very similar values; see Table 1) and the DOM source (divided experimentally into 3 categories; see Table 1). DOM sources comparable in salinity to the microbial community source appeared to have a greater potential for higher BMR values (Figure 9).

The dramatic decrease in fluorescence with irradiation for the riverine DOM (C1, C2), shown in the EEMS and PARAFAC data (Figures 6 & 7), is consistent with photochemical changes in the DOC composition of refractory riverine compounds to more biologically labile structures. This trend is confirmed by a slight increase in microbial growth when delivered to marine communities. Irradiation and the alteration of C1 and C2 does not, however, appear to significantly alter the large stimulating effect that riverine DOM, irradiated or not, has on the marine community (Figure 10). However, the lack of a stronger microbial response to irradiation

likely indicates that even prior to exposure, the concentration of labile DOC still exceeds any metabolic requirements of a marine community. Even after 48hrs of irradiation and fading of fluorescence in C1 and C2, the riverine DOM samples still exhibited higher levels of both components than were recorded at any other station sampled. Based on the 48 h trends, this increase would not be the case with pro-longed (weeks to months) exposure to solar radiation as the plume proceeds away from the river source.

The low salinity plume water was used as an inoculum in a variety of experiments and, accordingly, exhibited a variety of microbial responses. The general trend for these experiments was to increase BMR in the first six hours of DOM irradiation compared to next six hours (12 h total exposure) (Figure 3, 11). This result could be due to a sequential photochemical creation and destruction of labile organic molecules, with labile intermediates being created after a short irradiation, but consequently being destroyed as the exposure continued (Münster 1993). These unanticipated microbial results are consistent with the fluorescence patterns found for the LSP irradiation results as seen in the PARAFAC data (Figures 5-8). After an initial increase in C2 and C3, longer irradiation times caused both components to decrease. One interpretation of these patterns is that C1 fluorophores are initially photochemically altered into fragments that PARAFAC categorized as C2 or perhaps even C3. Humic acid, however, encompasses a large number of diverse compounds, structures, and spatial orientations, and thus the resulting unique UV breakdown products, along with their optical characteristics, are almost impossible to predict (Allard et al. 1994, Frimmel 1994, Corin et al. 1996).

For experiment LS1 in which the low salinity plume DOM (Stn6_2011) was evaluated for lability using the marine community from Stn9_2011, a greater BMR was observed in the mixed seawater than was seen for either source evaluated without mixing or filtering. The metabolic ratio was further increased with irradiation, but not to the same level observed after the addition of DOM from Stn6_2011 (Figure 3).

In a similar experiment, a Station 6 sample was aged for a week in the dark at constant temperature with its endemic bacterial community. Its resulting lability was assessed using a marine microbial community from Station 24 (similar to Station 9). While the un-filtered, unmixed, whole water BMR measurements were comparable to those obtained in the similar samples with fresh DOM, the results were unique in others ways. As expected, the non-irradiated mixture yielded significantly lower BMR values than both the natural and fresh DOM source waters. After 6 h of irradiation, however, the stimulation effect (on production and BMR) appeared to again be comparable to the natural water from the 2012 Station 6, a trend also seen after 12 h of irradiation. If the natural microbial community removed the biologically labile material during the aging period, much of the non-labile DOM must have remained photo-labile, creating new biologically labile material with exposure to solar radiation. Another possibility is that the microbial community could have created new photochemically reactive compounds from the labile DOC used during the dark incubation (Amon and Benner 1996a).

The sub-plume microbial community (Stn13_2011) responded differently than the surface communities when provided with low salinity plume water as its carbon source. While the introduction of the LSP DOM resulted in increased respiration, there was less of an increase than

observed in the surface community response (Stn9_2011) (Table 2) (Figure 11). There was also less of a stimulating effect in bacterial production values when compared to the surface waters. These factors lead to a 10% lower BMR in the sub-plume community than the surface communities. This effect is somewhat surprising since the DOM source water sampled for this experiment was in closer in proximity to the sub-plume community than what was used in the other pairings. With irradiation, production and respiration actually decreased by approximately 10% after 6 h of irradiation. There was an increase in respiration and production rates after the 12 h exposure, but only slightly above the rates found in the non-irradiated experiment. The introduction and subsequent irradiation of low salinity, high CDOM water did not have a significant stimulating effect on the sub-plume community when compared to the effect found on the surface communities. This result may represent a sub-plume community that is not adapted to take advantage of the irradiation products generated from the surface DOM, or alternatively, that simply started with less efficient utilization pathways than surface communities and, if incubated longer with irradiated products, the total effect may have been similar to surface communities.

The high salinity DOM sources generally did not stimulate microbial communities in the absence of irradiation. This result was true for the side-by-side high salinity plume edge sites, Station 26Brown and Station 26Blue. After 6 h of irradiation, BMR values calculated from the side-by-side stations were enhanced to levels comparable to other low salinity DOM experiments (Figure 4). The production levels for this pairing were the highest found in this study. As both Station 26 sites were most likely periodically mixed with one another, the microbial community could have had DOC pathways that are ready to rapidly respond to the photochemical constituents

found in either site. The lack of response to the HS DOM without irradiation may reflect dilution of the lower salinity DOM water with less nutrient rich water. This effect might also explain the results observed when high salinity marine DOM (Stn5a_2012) is provided to a low salinity plume community (Stn6_2012). The mixed, non-irradiated sample had approximately the same average respiration rates and production rates compared to other treatments. There was an increase in all responses with irradiation, but it never reached the levels attained by the community when using the carbon sources from the natural low salinity plume DOM. Our results therefore confirm previous findings, that even in the clearest of water, with low CDOM absorbance to drive photochemistry, there is potential for photochemical transformations that alter microbial carbon cycling (Vähätalo and Wetzel 2004).

Relatively little is understood about the specific interactions between photochemical and microbial processing of DOM and reciprocal effects on lability. There have been numerous attempts to investigate this linkage, but the results have been vastly dissimilar and no consistent universal effect has been identified. 50% of the studies reviewed by Mopper and Kieber (2002) irradiated the microbial community indicator along with the DOM source, which could affect the abilities of the microbes to metabolize any organic matter. An additional 30% of these studies used artificial DOM or amended the DOM by adding lignin, fatty acids, or bovine serum albumin. These additions would test the microbial community but not necessarily mimic natural conditions or transformations of natural DOM. These two groupings leave only 12 of the 61 studies that Mopper and Kieber (2002) reviewed comparable to natural PCML systems, thus casting doubt onto the relevance of many results compared to this study.

Our research was designed to address the potential pitfall of assuming static conditions in a non-static environment. The microbial responses shown here indicate the need for careful consideration in choosing a biolability indicator community for use in any photochemical microbial linkage research, but particularly so in a dynamic system such as the Amazon River plume. The work by Rochelle-Newall et al. (2004) was done in the 145 km long River Guden, with an average discharge of $35 m^3 s^{-1}$, and a drainage basin of less than 400,00 km^2 (Thodsen 2007). Results showed an increase in the functional response of seawater communities provided with DOM, but not a strong difference between different origins of this DOM (fresh water, at the end of an fjord estuary, or seawater collected at some unspecified distance from the river mouth). While this study did provide proof of photochemical enhancement of DOM and the importance of community choice, possibly due to the nature of their river system, differences between the freshwater and seawater DOM were not dramatic enough to provoke a measureable difference in microbial response. Also, had the study site been further from the river, a greater effect might have been seen. A similar argument could be made for the work by Piccini et al. (2009), in that the static nature of their lagoonal sample site may confound valid comparison to the dynamic Amazon system.

The work by Abboudi et al (2008) seems to strengthen the argument that static and dynamic systems may require different approaches. They found a 120% increase in bacterial growth efficiency in a coastal site, located near a small river, but a 20-40% decrease in the more stable lagoonal waters, all as compared to respective dark controls. These experiments were run with inoculums from the same source, which may have been different from when the DOM was collected. Regardless, the range of responses in this study were as dramatic as those found

across the entire PCML literature. When looking at dynamic sites similar to the Amazon, such as the Congo and the Mississippi, these results from Abboudi et al. (2008) might be used to argue for a need to examine PCML interactions in a manner similar to the study reported here.

Work done by Spencer et al. (2009, 2010) follows the chemical aspects of PCML, but assigns no direct measurement to the microbial activity itself, merely reporting the observed changes in the DOM. This narrow focus might lead to an oversimplification of the system and thus miss some of the intricacies and balances between the photo- and biologically labile DOM pools, and miss entirely the DOM pool that is both. A similar chemical bias is found in the Benner and Opsahl (2001) Mississippi River study. All these dynamic riverine systems showed a decrease of terrestrial DOM with irradiation, but the microbial response was less clear, perhaps due to the microbial inclusion in the irradiated samples or the lack of direct microbial measurement. PCML research has the potential to further elucidate the complex questions regarding the fate and transformation of terrestrial matter in the marine systems. In the interplay between the microbial consumption and the photochemical transformation of riverine DOM, both processes must be studied simultaneously. Future attempts to elucidate the synergistic effect of both processes on the DOM pool will provide a distinct challenge for photochemists and microbiologists together to further investigate the fate of terrestrial DOM delivered by rivers into the marine environment.

REFERENCES

Abboudi, M., W. Jeffrey, J. F. Ghiglione, M. Pujo-Pay, L. Oriol, R. Sempere, B. Charrière, and F. Joux. 2008. Effects of photochemical transformations of dissolved organic matter on bacterial metabolism and diversity in three contrasting coastal sites in the northwestern Mediterranean Sea during summer. Microbial ecology **55**:344-357.

Allard, B., H. Boren, C. Pettersson, and G. Zhang. 1994. Degradation of humic substances by UV irradiation. Environment International **20**:97-101.

Amon, R. and R. Benner. 1996a. Photochemical and microbial consumption of dissolved organic carbon and dissolved oxygen in the Amazon River system. Geochimica Et Cosmochimica Acta **60**:1783-1792.

Amon, R. M. W. and R. Benner. 1996b. Photochemical and microbial consumption of dissolved organic carbon and dissolved oxygen in the Amazon River system. Geochimica Et Cosmochimica Acta **60**:1783-1792.

Bauer, J. and T. Bianchi, editors. 2011. Dissolved Organic Carbon Cycling and Transformation. Waltham: Academic Press.

Benner, R. and S. Opsahl. 2001. Molecular indicators of the sources and transformations of dissolved organic matter in the Mississippi river plume. Organic Geochemistry **32**:597-611.

Berggren, M., J.-F. Lapierre, and P. A. del Giorgio. 2011. Magnitude and regulation of bacterioplankton respiratory quotient across freshwater environmental gradients. The ISME journal **6**:984-993.

Bertilsson, S. and L. J. Tranvik. 1998. Photochemically produced carboxylic acids as substrates for freshwater bacterioplankton. Limnology and Oceanography:885-895.

Briand, E., O. Pringault, S. Jacquet, and J.-P. Torreton. 2004. The use of oxygen microprobes to measure bacterial respiration for determining bacterioplankton growth efficiency. Limnology and Oceanography: Methods **2**:406-416.

Bro, R. 1997. PARAFAC. Tutorial and applications. Chemometrics and intelligent laboratory systems **38**:149-171.

Coble, P. G. 1996. Characterization of marine and terrestrial DOM in seawater using excitation-emission matrix spectroscopy. Marine Chemistry **51**:325-346.

Cooley, S. and P. Yager. 2006. Physical and biological contributions to the western tropical North Atlantic Ocean carbon sink formed by the Amazon River plume. Journal of Geophysical Research **111**:C08018.

Corin, N., P. Backlund, and M. Kulovaara. 1996. Degradation products formed during UV-irradiation of humic waters. Chemosphere **33**:245-255.

Dagg, M., R. Benner, S. Lohrenz, and D. Lawrence. 2004. Transformation of dissolved and particulate materials on continental shelves influenced by large rivers: plume processes. Continental shelf research **24**:833-858.

del Giorgio, P. A. and J. J. Cole. 1998. Bacterial growth efficiency in natural aquatic systems. Annual Review of Ecology and Systematics:503-541.

Del Vecchio, R. and A. Subramaniam. 2004. Influence of the Amazon River on the surface optical properties of the western tropical North Atlantic Ocean. Journal of Geophysical Research **109**:C11001.

DeLong, E. F. 2009. The microbial ocean from genomes to biomes. Nature **459**:200-206.

Ducklow, H. 1992. Oceanic bacterial production. Advances in microbial ecology **12**:113-181.

Frimmel, F. H. 1994. Photochemical aspects related to humic substances. Environment International **20**:373-385.

Fuhrman, J. A., J. A. Steele, I. Hewson, M. S. Schwalbach, M. V. Brown, J. L. Green, and J. H. Brown. 2008. A latitudinal diversity gradient in planktonic marine bacteria. Proceedings of the National Academy of Sciences **105**:7774-7778.

Garvine, R. W. 1995. A dynamical system for classifying buoyant coastal discharges. Continental shelf research **15**:1585-1596.

Gasol, J. M. and P. A. Del Giorgio. 2000. Using flow cytometry for counting natural planktonic bacteria and understanding the structure of planktonic bacterial communities. Scientia Marina **64**:197-224.

Gattuso, J. P., M. Frankignoulle, and R. Wollast. 1998. Carbon and carbonate metabolism in coastal aquatic ecosystems. Annual Review of Ecology and Systematics:405-434.

Geyer, W., R. Beardsley, J. Candela, B. Castro, R. Legeckis, S. Lentz, R. Limeburner, L. Miranda, and J. Trowbridge. 1991. The physical oceanography of the Amazon outflow. Oceanography **4**:8-15.

Gjessing, E. T. and T. Källqvist. 1991. Algicidal and chemical effect of uv-radiation of water containing humic substances. Water research **25**:491-494.

Hedges, J., R. Keil, and R. Benner. 1997. What happens to terrestrial organic matter in the ocean? Organic Geochemistry **27**:195-212.

Hedges, J. I., P. G. Hatcher, J. R. Ertel, and K. J. Meyers-Schulte. 1992. A comparison of dissolved humic substances from seawater with Amazon River counterparts by< sup> 13</sup> C-NMR spectrometry. Geochimica Et Cosmochimica Acta **56**:1753-1757.

Hernes, P. J. and R. Benner. 2003. Photochemical and microbial degradation of dissolved lignin phenols: Implications for the fate of terrigenous dissolved organic matter in marine environments. Journal of Geophysical Research **108**:3291.

Isobe, A. 2005. Ballooning of river-plume bulge and its stabilization by tidal currents. Journal of Physical Oceanography **35**:2337-2351.

Kieber, D. J. 2000. Photochemical production of biological substrates. The Effects of UV Radiation in the Marine Environment:130-148.

Kieber, D. J. and K. Mopper. 1987. Photochemical formation of glyoxylic and pyruvic acids in seawater. Marine Chemistry **21**:135-149.

Kirchman, D. 2001. Measuring bacterial biomass production and growth rates from leucine incorporation in natural aquatic environments. Methods in microbiology **30**:227-237.

Kourafalou, V. H., L. Y. Oey, J. D. Wang, and T. N. Lee. 1996. The fate of river discharge on the continental shelf 1. Modeling the river plume and the inner shelf coastal current. Journal of Geophysical Research **101**:3415-3434.

Kowalczuk, P., M. J. Durako, H. Young, A. E. Kahn, W. J. Cooper, and M. Gonsior. 2009. Characterization of dissolved organic matter fluorescence in the South Atlantic Bight with use of PARAFAC model: Interannual variability. Marine Chemistry **113**:182-196.

Labasque, T., C. Chaumery, A. Aminot, and G. Kergoat. 2004. Spectrophotometric Winkler determination of dissolved oxygen: re-examination of critical factors and reliability. Marine Chemistry **88**:53-60.

Lemée, R., E. Rochelle-Newall, F. Van Wambeke, M. Pizay, P. Rinaldi, and J. Gattuso. 2002. Seasonal variation of bacterial production, respiration and growth efficiency in the open NW Mediterranean Sea. Aquatic microbial ecology **29**:227-237.

Limeburner, R., R. C. Beardsley, I. D. Soares, S. J. Lentz, and J. Candela. 1995. Lagrangian flow observations of the Amazon River discharge into the North Atlantic. Journal of Geophysical Research **100**:2401-2415.

Ludwig, W. and J. L. Probst. 1998. River sediment discharge to the oceans; present-day controls and global budgets. American Journal of Science **298**:265-295.

Mackenzie, F. T., A. J. Andersson, R. S. Arvidson, M. W. Guidry, and A. Lerman. 2011. Land–sea carbon and nutrient fluxes and coastal ocean CO2 exchange and acidification: Past, present, and future. Applied Geochemistry **26, Supplement**:S298-S302.

Massicotte, P. and J.-J. Frenette. 2011. Spatial connectivity in a large river system: resolving the sources and fate of dissolved organic matter. Ecological Applications **21**:2600-2617.

McKnight, D. M., E. W. Boyer, P. K. Westerhoff, P. T. Doran, T. Kulbe, and D. T. Andersen. 2001. Spectrofluorometric characterization of dissolved organic matter for indication of precursor organic material and aromaticity. Limnology and Oceanography:38-48.

Miller, W. L. and M. A. Moran. 1997. Interaction of photochemical and microbial processes in the degradation of refractory dissolved organic matter from a coastal marine environment. Limnology and Oceanography:1317-1324.

Miller, W. L. and R. G. Zepp. 1995. Photochemical production of dissolved inorganic carbon from terrestrial organic matter: Significance to the oceanic organic carbon cycle. Geophysical Research Letters **22**:417-420.

Mobed, J. J., S. L. Hemmingsen, J. L. Autry, and L. B. McGown. 1996. Fluorescence characterization of IHSS humic substances: total luminescence spectra with absorbance correction. Environmental science & technology **30**:3061-3065.

Mopper, K. and D. J. Kieber, editors. 2002. Photochemistry and the cycling of carbon, sulfur, nitrogen and phosphorus. Academic Press.

Muller-Karger, F., P. Richardson, and D. McGillicuddy. 1995. On the offshore dispersal of the Amazon's Plume in the North Atlantic: Comments on the paper by A. Longhurst,“Seasonal cooling and blooming in tropical oceans”. Deep Sea Research Part I: Oceanographic Research Papers **42**:2127-2137.

Münster, U. 1993. Concentrations and fluxes of organic carbon substrates in the aquatic environment. Antonie van Leeuwenhoek **63**:243-274.

Murphy, K. R., C. A. Stedmon, T. D. Waite, and G. M. Ruiz. 2008. Distinguishing between terrestrial and autochthonous organic matter sources in marine environments using fluorescence spectroscopy. Marine Chemistry **108**:40-58.

Nash, J. D. and J. N. Moum. 2005. River plumes as a source of large-amplitude internal waves in the coastal ocean. Nature **437**:400-403.

Nichols, D. S. 2006. Prokaryotes and the input of polyunsaturated fatty acids to the marine food web. FEMS Microbiology Letters **219**:1-7.

Oltman, R. E. 1968. Reconnaissance investigations of the discharge and water quality of the Amazon River. USGS, Washington, D.C.

Pommier, T., B. Canbäck, L. Riemann, K. Boström, K. Simu, P. Lundberg, A. Tunlid, and Å. Hagström. 2006. Global patterns of diversity and community structure in marine bacterioplankton. Molecular ecology **16**:867-880.

Reinthaler, T., C. Winter, and G. J. Herndl. 2005. Relationship between bacterioplankton richness, respiration, and production in the southern North Sea. Applied and environmental microbiology **71**:2260-2266.

Remington, S., A. Krusche, and J. Richey. 2011. Effects of DOM photochemistry on bacterial metabolism and CO 2 evasion during falling water in a humic and a whitewater river in the Brazilian Amazon. Biogeochemistry **105**:185-200.

Richey, J. E., R. L. Victoria, E. Salati, and B. R. Forsberg. 1991. The biogeochemistry of a major river system: The Amazon case study. Biogeochemistry of major world rivers **42**:57-74.

Robinson, C. and P. l. B. Williams. 2005. Respiration and its measurement in surface marine waters. Respiration in aquatic ecosystems:148-181.

Rochelle-Newall, E. J., M. D. Pizay, J. J. Middelburg, H. T. S. Boschker, and J. P. Gattuso. 2004. Degradation of riverine dissolved organic matter by seawater bacteria. Aquatic microbial ecology **37**:9-22.

Rodriguez-Brito, B., L. L. Li, L. Wegley, M. Furlan, F. Angly, M. Breitbart, J. Buchanan, C. Desnues, E. Dinsdale, and R. Edwards. 2010. Viral and microbial community dynamics in four aquatic environments. The ISME journal **4**:739-751.

Smith, D. C. and F. Azam. 1992. A simple, economical method for measuring bacterial protein synthesis rates in seawater using 3H-leucine. Mar. Microb. Food Webs **6**:107-114.

Spencer, R. G., P. J. Hernes, R. Ruf, A. Baker, R. Y. Dyda, A. Stubbins, and J. Six. 2010. Temporal controls on dissolved organic matter and lignin biogeochemistry in a pristine tropical river, Democratic Republic of Congo. Journal of Geophysical Research: Biogeosciences (2005–2012) **115**.

Spencer, R. G., A. Stubbins, P. J. Hernes, A. Baker, K. Mopper, A. K. Aufdenkampe, R. Y. Dyda, V. L. Mwamba, A. M. Mangangu, and J. N. Wabakanghanzi. 2009. Photochemical degradation of dissolved organic matter and dissolved lignin phenols from the Congo River. Journal of Geophysical Research **114**:G03010.

Stedmon, C. A. and S. Markager. 2005. Tracing the Production and Degradation of Autochthonous Fractions of Dissolved Organic Matter by Fluorescence Analysis. Limnology and Oceanography **50**:1415-1426.

Stedmon, C. A., S. Markager, and R. Bro. 2003. Tracing dissolved organic matter in aquatic environments using a new approach to fluorescence spectroscopy. Marine Chemistry **82**:239-254.

Thodsen, H. 2007. The influence of climate change on stream flow in Danish rivers. Journal of Hydrology **333**:226-238.

Vähätalo, A. V. and R. G. Wetzel. 2004. Photochemical and microbial decomposition of chromophoric dissolved organic matter during long (months–years) exposures. Marine Chemistry **89**:313-326.

Wetzel, R. G., P. G. Hatcher, and T. S. Bianchi. 1995. Natural photolysis by ultraviolet irradiance of recalcitrant dissolved organic matter to simple substrates for rapid bacterial metabolism. Limnology and Oceanography:1369-1380.

Williams, P. l. B. and P. A. del Giorgio, editors. 2005. Respiration in aquatic ecosystems: History and background. Oxford Univeristy Press.

Wiseman, W. and R. Garvine. 1995. Plumes and coastal currents near large river mouths. Estuaries and Coasts **18**:509-517.

Wollast, R. 1998. Evaluation and comparison of the global carbon cycle in the coastal zone and in the open ocean. The sea **10**:213-252.

Yamashita, Y., N. Maie, H. Briceño, and R. Jaffé. 2010. Optical characterization of dissolved organic matter in tropical rivers of the Guayana Shield, Venezuela. Journal of Geophysical Research **115**:G00F10.

Yankovsky, A. E. and D. C. Chapman. 1997. A Simple Theory for the Fate of Buoyant Coastal Discharges. Journal of Physical Oceanography **27**:1386-1401.

Zafiriou, O. C. 1977. Marine organic photochemistry previewed. Marine Chemistry **5**:497-522.

Zepp, R. G., W. M. Sheldon, and M. A. Moran. 2004. Dissolved organic fluorophores in southeastern US coastal waters: correction method for eliminating Rayleigh and Raman scattering peaks in excitation–emission matrices. Marine Chemistry **89**:15-36.

Zhukova, N. V. and V. I. Kharlamenko. 1999. Sources of essential fatty acids in the marine microbial loop. Aquatic microbial ecology **17**:153-157.

Table 1: Experimental Groupings and Sampling Station Characteristics

Experiemental Group	Subset	DOM Source (Yr_Stn)	Salinity (psu)	Temp (˚C)	1% PAR Depth (m)	Sample Depth (m)	Fluorescence (mg/m3)	Community Source (Yr_Stn)	Salinity (psu)	Temp (˚C)	1% PAR Depth (m)	Sample Depth (m)	Fluorescence (mg/m3)
Riverine DOM		**2012_Stn 10**	0.24	28.58	0	2.46	1.956	**2012_Stn 15**	36.47	28.4	69	3.91	0.243
Low Salinity DOM	**1**	**2011_Stn 6**	27.96	28.55	21.5	2.07	0.617	**2011_Stn 9**	34.89	28.86	45	2	0.082
	2	**2011_Stn 6 (Aged)**	27.96	28.55	21.5	2.07	0.617	**2011_Stn 24**	34.06	30.02	70.41	2.5	0.074
	3	**2011_Stn 11**	27.84	29.73	24.73	2.04	0.446	**2011_Stn 13 (Sub)**	35.38	28.5	55.8	13.6	0.114
High Salinity DOM	**1**	**2011_Stn 26Brown**	34.7	28.9	58.3	2.5	0.098	**2011_Stn 26Blue**	34.89	28.86	84.4	2.32	0.080
	2	**2012_Stn 5a**	34.64	28.5	52.4	4.5	0.186	**2012_Stn 6**	32.45	27.75	32	3.11	0.334

Table 2: Microbial Responses (Respiration & Production Values)

Experiment by DS (additional info)	Sample Type (filtration) [hrs irradiated]	Average Respiration Rate (nmol C/L/hr)	Respiration Standard Deviation (n=3)	Average Production Rate (nmol C/L/hr)	Production Standard Deviation (n=3)
Riverine	DS (whole)	597.1926723	12.5944822	122.5557416	11.8974608
	DS (0.2)	27.80732772	3.80328369	0.786631747	0.57554381
	CS (whole)	283.3283689	8.0450423	51.3082777	3.52269228
	CS (3)	202.83046	9.81268288	38.8320419	9.23599511
	CS (0.2)	22.92120419	1.17404608	0.507140052	1.8269633
	CS (3) + CS (0.2)	138.3879	7.94093701	24.83172261	6.00674611
	DS (0.2)[0] + CS (3)	538.8232181	9.81268288	125.5832089	17.6839957
	DS (0.2)[6] + CS (3)	573.5940921	6.26883681	141.6492635	21.8060876
	DS (0.2)[12] + CS (3)	521.3980477	9.14034189	143.4316026	12.610086
	DS (0.2)[18] + CS (3)	519.2913304	12.0404053	192.2828117	20.8045477
	DS (0.2)[24] + CS (3)	541.1863825	9.16940424	315.2567923	37.4975816
Low Salinity 1	DS (whole)	525.4394938	8.54053681	130.200217	2.55799968
	CS (whole)	372.0422871	11.632281	123.1665273	22.1303432
	CS (3)	362.9680849	12.0637028	33.98537172	0.72246677
	DS (0.2)[0] + CS (3)	609.8461187	9.57153265	478.0335891	22.1303432
	DS (0.2)[6] + CS (3)	722.9951115	8.02835356	673.2114059	36.1103709
	DS (0.2)[12] + CS (3)	814.1660551	4.91845076	744.8727713	34.8057711
Low Salinity 2 (Aged DS)	DS (whole)	525.4394938	8.54053681	130.200217	2.55799968
	DS (0.2)	51.98263047	6.48089818	0.402294681	0.03474589
	CS (whole)	465.8110468	11.3407201	103.0188256	9.05812093
	CS (3)	276.2592436	8.04039603	39.03021445	3.42041895
	DS (0.2)[0] + CS (3)	544.9391316	16.9775944	343.2304366	11.0325379
	DS (0.2)[6] + CS (3)	656.8259192	5.86039728	558.5626099	17.4020343
	DS (0.2)[12] + CS (3)	759.8533939	5.71746076	927.8570655	31.8701961
Low Salinity 3 (Sub-plume CS)	DS (whole)	650.5071767	5.89275346	169.2602821	6.77529025
	CS (whole)	396.9013865	11.3485668	81.92428438	3.41024781
	DS (0.2)[0] + CS (3)	632.2583631	9.14489367	286.5973487	6.12522491
	DS (0.2)[6] + CS (3)	794.3083465	4.79848854	188.5666199	8.97849882
	DS (0.2)[12] + CS (3)	732.6575236	14.978008	376.7557879	18.9655657
High Salinity 1 (Plume Edge)	DS (whole)	766.1997396	2.74312252	282.8872938	22.728137
	DS (0.2)	63.47741862	6.51135929	3.343162605	0.30515456
	CS (whole)	416.2320087	5.9473354	94.67371773	4.37076796
	CS (3)	319.4537865	9.56677205	27.12789397	0.70499209
	DS (0.2)[0] + CS (3)	605.4628447	14.3843526	79.08482845	3.70933716
	DS (0.2)[6] + CS (3)	1059.901652	10.8442667	1329.03	35.34
	DS (0.2)[12] + CS (3)	980.7266245	9.62315568	1245.396568	53.7489482
High Salinity 2 (Exp Design Reversal)	DS (whole)	266.3662174	6.39278922	79.7643137	5.31762091
	DS (0.2)	18.63090957	8.098882	0.786631747	1.76979075
	CS (whole)	474.0663108	10.452947	428.3701913	23.2947004
	DS (0.2)[0] + CS (3)	366.3723289	11.1154915	228.3158923	21.2004386
	DS (0.2)[6] + CS (3)	680.6269701	10.4715533	458.6062038	44.2159409
	DS (0.2)[12] + CS (3)	698.735331	12.8901178	613.5555329	27.4164628

Relative (Post incubation-Pre incubation) rates for respiration and production and standard deviations for each triplicate, DS = DOM Source Water, CS = Microbial Community Source Water

Table 3: Bacterial Abundance Data

Experiment by DS (additional info)	Sample Type (filtration) {hrs incubated}	Average Bactrial Cell Count	Standard Deviation (n=4)
Riverine	DS (whole)	5.88E+05	3.48E+05
	DS (3)	1.28E+06	2.39E+05
	CS (whole)	6.34E+05	3.44E+03
	CS (3)	6.59E+05	7.36E+03
Low Salinity 1	DS (whole)	1.25E+06	6.13E+04
	CS (whole)	5.26E+05	3.94E+04
Low Salinity 2 (Aged DS)	CS (whole)	5.33E+05	1.85E+04
	CS (3)	5.18E+05	6.24E+04
Low Salinity 3 (Sub-plume CS)	DS (whole)	1.76E+06	2.34E+05
	CS (whole)	6.66E+05	5.94E+04
High Salinity 1 (Plume Edge)	DS (whole)	7.27E+05	6.42E+04
	DS (3)	7.59E+05	4.09E+04
	CS (whole)	8.60E+05	1.17E+05
	CS (3) {0}	8.83E+05	1.41E+04
	CS (3) {24}	3.25E+06	2.90E+05
High Salinity 2 (Exp Design Reversal)	DS (whole)	9.14E+05	5.96E+04
	DS (3)	8.49E+05	2.43E+04
	DS (0.2) {0}	2.01E+05	1.59E+04
	DS (0.2) {24}	2.41E+05	9.24E+03
	CS (whole)	6.44E+05	3.44E+04
	CS (3) {0}	4.10E+05	3.74E+04
	CS (3) {24}	5.32E+05	2.05E+04

Bacterial Abundances for Source Waters with Filtration, and Incubations (in the High Salinity Experiments), Standard Deviations are calculated from two runs of duplicate preserved vials from same sample for total n=4, DS = DOM Source Water, CS = Microbial Community Source Water

Table 4: PARAFAC Components Literature Comparison

Component	Excitation Maximum (nm)/ Emission Maximum (nm)	Potential Source Description (Reference)
1	<250 (320) / 436	Terrestrial humic, microbially transformable, UV&Visible light sensitive Component 1: <260 (315)/447 (Yamashita et al. 2010) Component 1: 250/452 (Kowalczuk et al. 2009) P1: <260 (310)/414 (Murphy et al. 2008) Component 1: 250/448 (Stedmon & Markager 2005) Component 1: 240/436 (Stedmon et al. 2003) “A” peak (Coble 1996)
2	275 (390) / 458	Terrestrial humic, microbially transformable, UV light sensitive Component 2: <260 (370)/>500 (Yamashita et al. 2010) Component 4: 270 (390)/508 (Kowalczuk et al. 2009) P3: <260 (380)/498 (Murphy et al. 2008) Component 2: 250 (385)/504 (Stedmon & Markager 2005) Component 3: 270 (360)/478 (Stedmon et al. 2003) “A” and “C” peaks (Coble 1996)
3	<250 (290) / 378	Microbial protein, polyphenol, tryptophan, algae-derived, UV light sensitive Component 4: <260 (370)/440 (Yamashita et al. 2010) Component 5: <260/325 (Yamashita et al. 2010) Component 6: 250 (290)/356 (Kowalczuk et al. 2009) P7: 280/342 (Murphy et al. 2008) Component 7: 280/344 (Stedmon & Markager 2005) "T" peak (Coble 1996)

Major EEMS Peaks associated with PARAFAC Components and Literature Comparisons for Components.

Table 5: Modeled Station Water Body Ages

Experiemental Group	Subset	DOM Source (Yr Stn)	Range of days from Mouth	Community Source (Yr Stn)	Range of days from Mouth	Apx Time between Stations (days)
Riverine DOM		**2012_Stn 10**	0-10	**2012_Stn 15**	n/a[1]	n/a[1]
Low Salinity DOM	**1**	**2011_Stn 6**	10-30	**2011_Stn 9**	20-40	10
	2	**2011_Stn 6 (Aged)**	17-37	**2011_Stn 24**	30-70	30
	3	**2011_Stn 11**	0-30	**2011_Stn 13 (Sub)**	n/a[2]	n/a[2]
High Salinity DOM	**1**	**2011_Stn 26Brown**	80-120	**2011_Stn 26Blue**	80-120	n/a[3]
	2	**2012_Stn 5a**	0-20	**2012_Stn 6**	0-10	n/a[4]

n/a[1] not enough floats arrived at 2012_Stn 15 to calculate

n/a[2] all floats on surface, 2011_Stn 13 was sub-plume

n/a[3] stations too close too differentiate with float data

n/a[4] the DOM source is down-plume from the community source (reversal experiment), so would be negative 10d

Data generated with HYCOM model (Victoria Coles, University of Maryland).

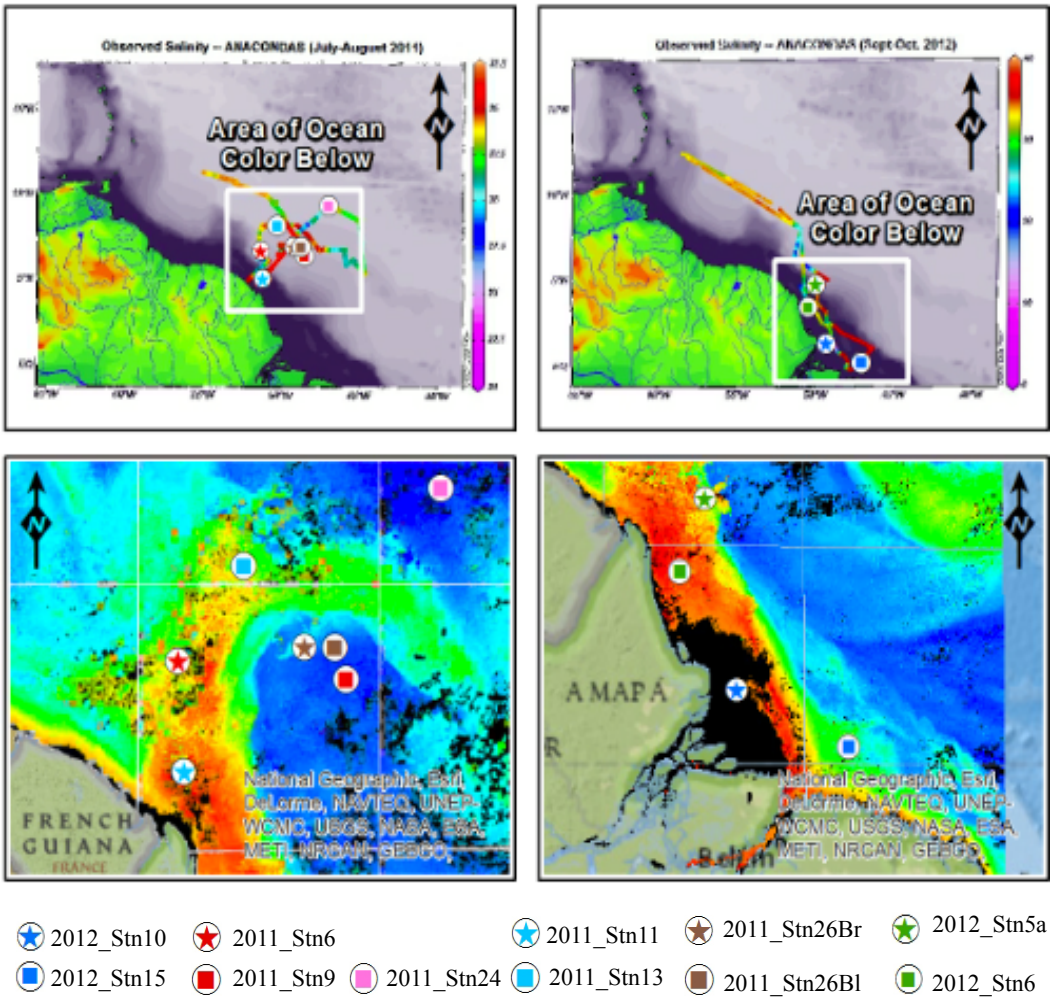

Figure 1: Location of Sample Sites.

Left Column displays cruise data from 2011, Right Column displays cruise data from 2012, Top Row shows ocean color, and Bottom Row shows salinity.

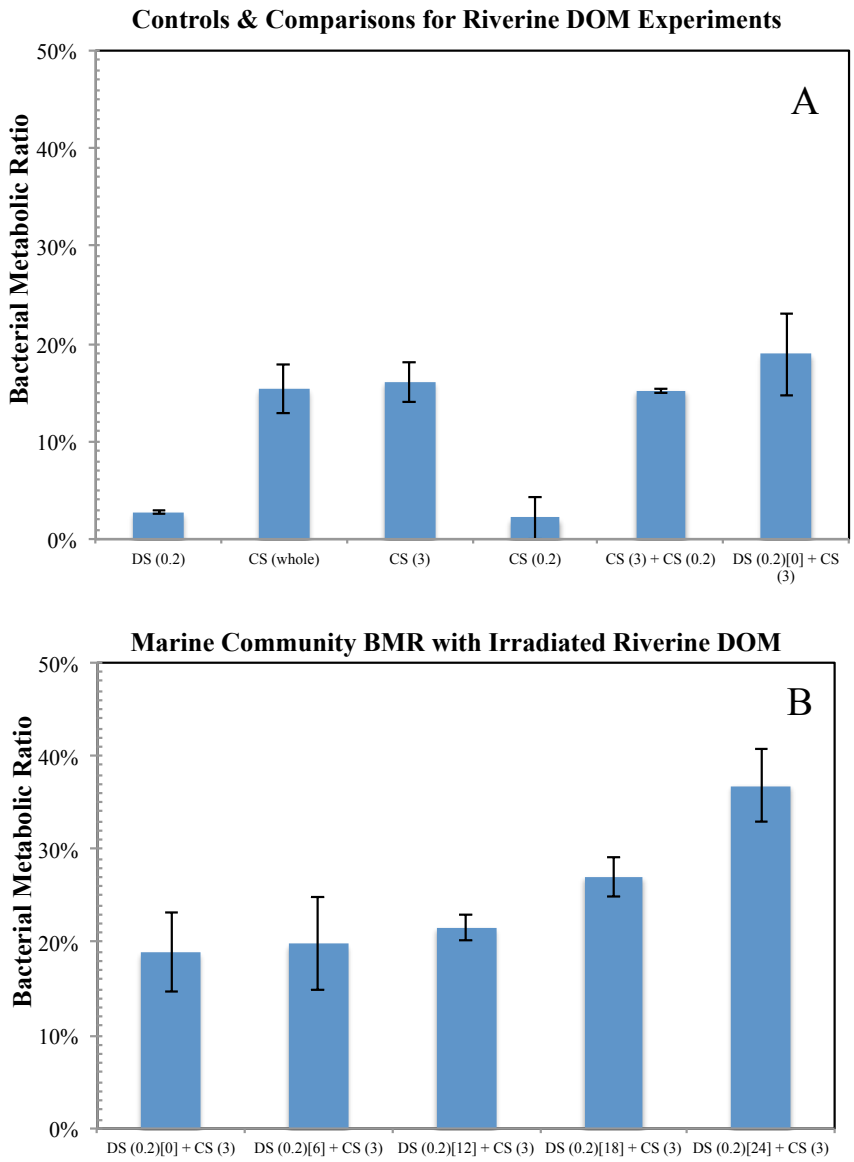

Figure 2: Riverine DOM Source: Bacterial Metabolic Ratios

Using a marine microbial community. **A**: Provides comparisons for unfiltered whole water, dilution effects (sample CS (3) and sample CS (0.2) vs sample CS (3) + CS (0.2)) **B**: Effects of irradiated riverine DOM on BMR of marine microbial community. Last Bar in A is same as first in B. *Format for Labels: Sample type (filtration in µm) [irradiation in h] DS = DOM Source Water, CS = Microbial Community Source Water*

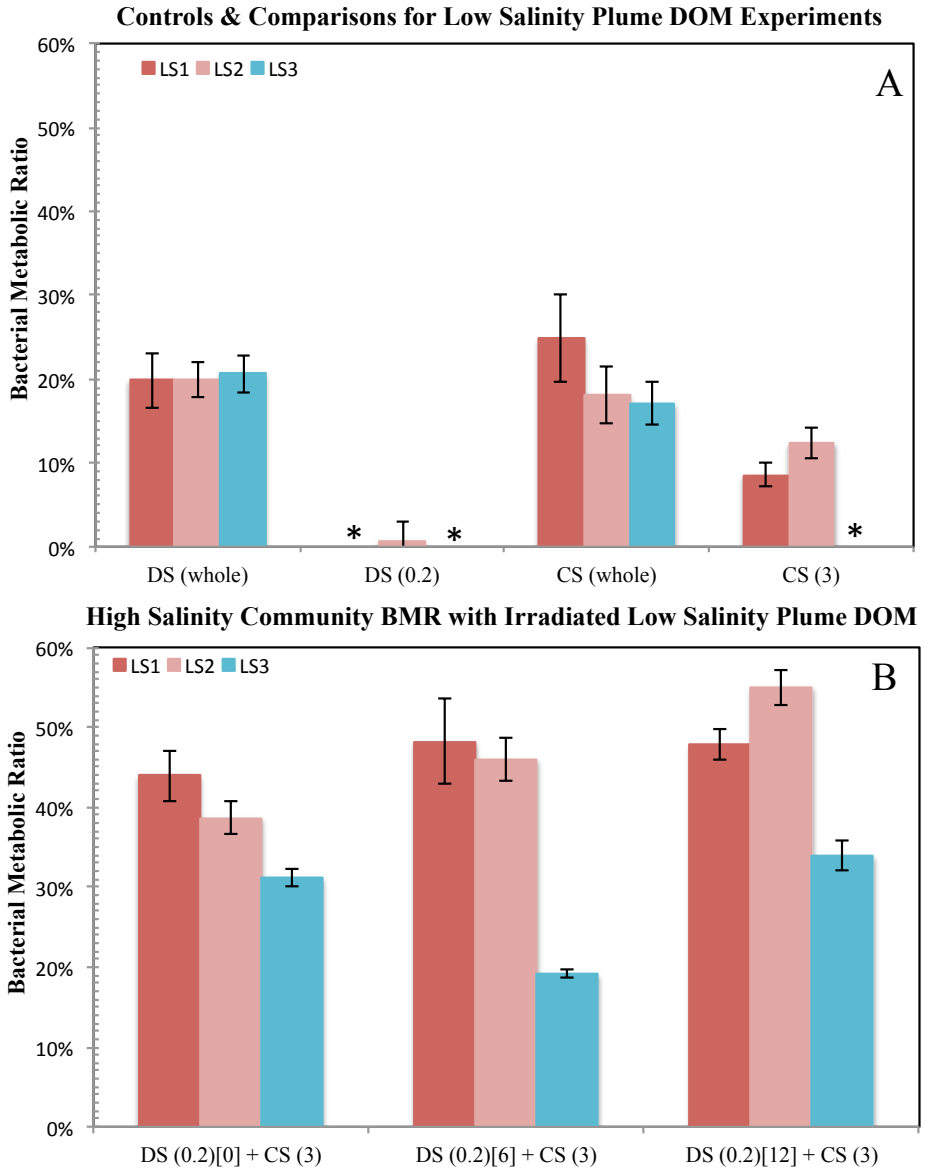

Figure 3: Low Salinity DOM Source: Bacterial Metabolic Ratios

Using a high salinity microbial community. A: Provides comparisons for unfiltered whole water. B: Effects of irradiated LSP DOM on BMR of high salinity microbial community.

*Format for Labels: Sample type (filtration in µm) [irradiation in h], *= No sample collected DS = DOM Source Water, CS = Microbial Community Source Water*

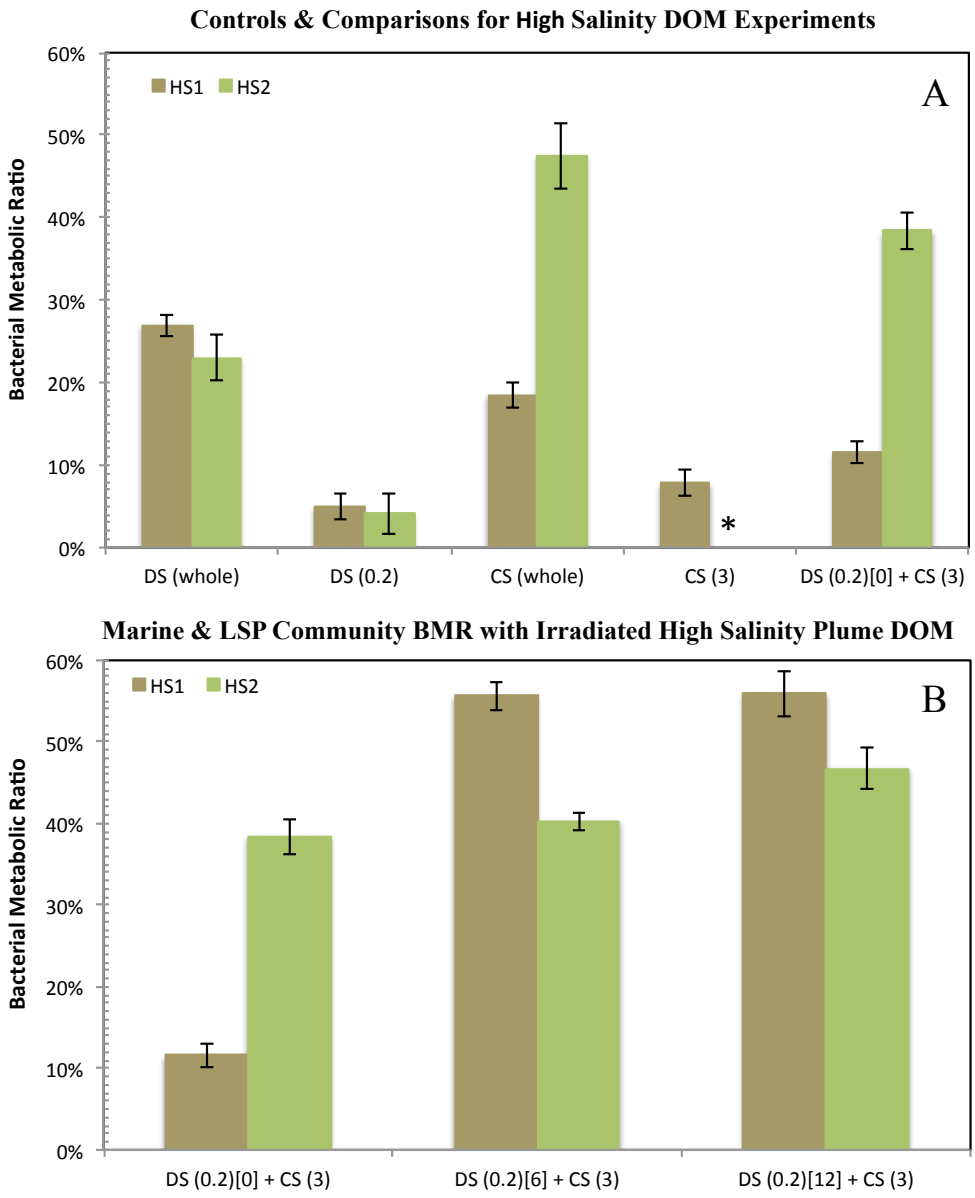

Figure 4: High Salinity DOM Source: Bacterial Metabolic Ratios

Using a high salinity microbial community and a Low Salinity Plume (LSP) community. **A:** Comparisons for unfiltered whole water. **B:** Effects of irradiated HS DOM on BMR of high salinity microbial community and a LSP community. *Format for Labels: Sample type (filtration in µm) [irradiation in h], *= No sample collected, DS = DOM Source Water, CS = Microbial Community Source Water*

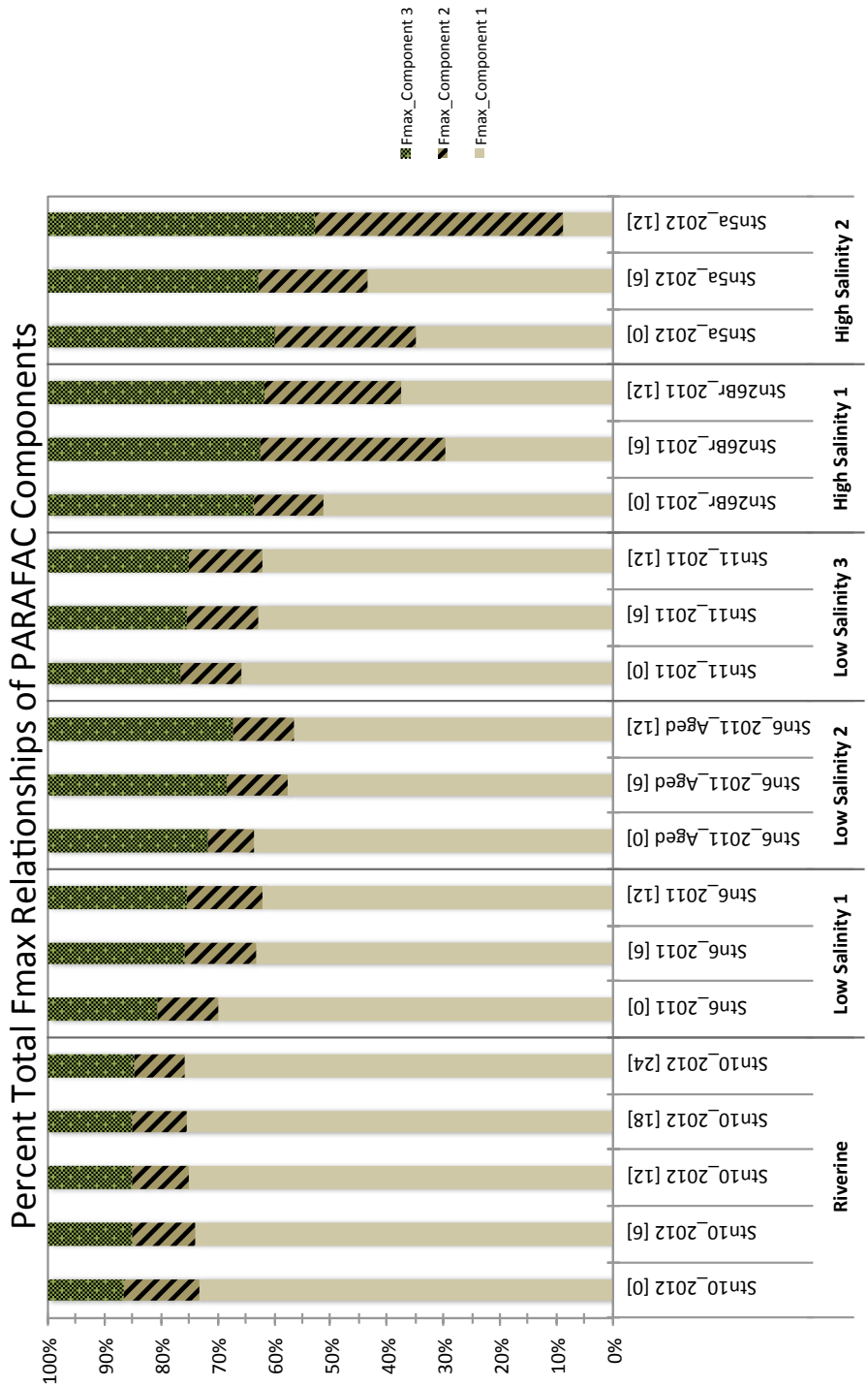

Figure 5: PARAFAC Component Ratios Over Irradiation

Contributions of each PARFAC component to the total Fmax generated by each sample

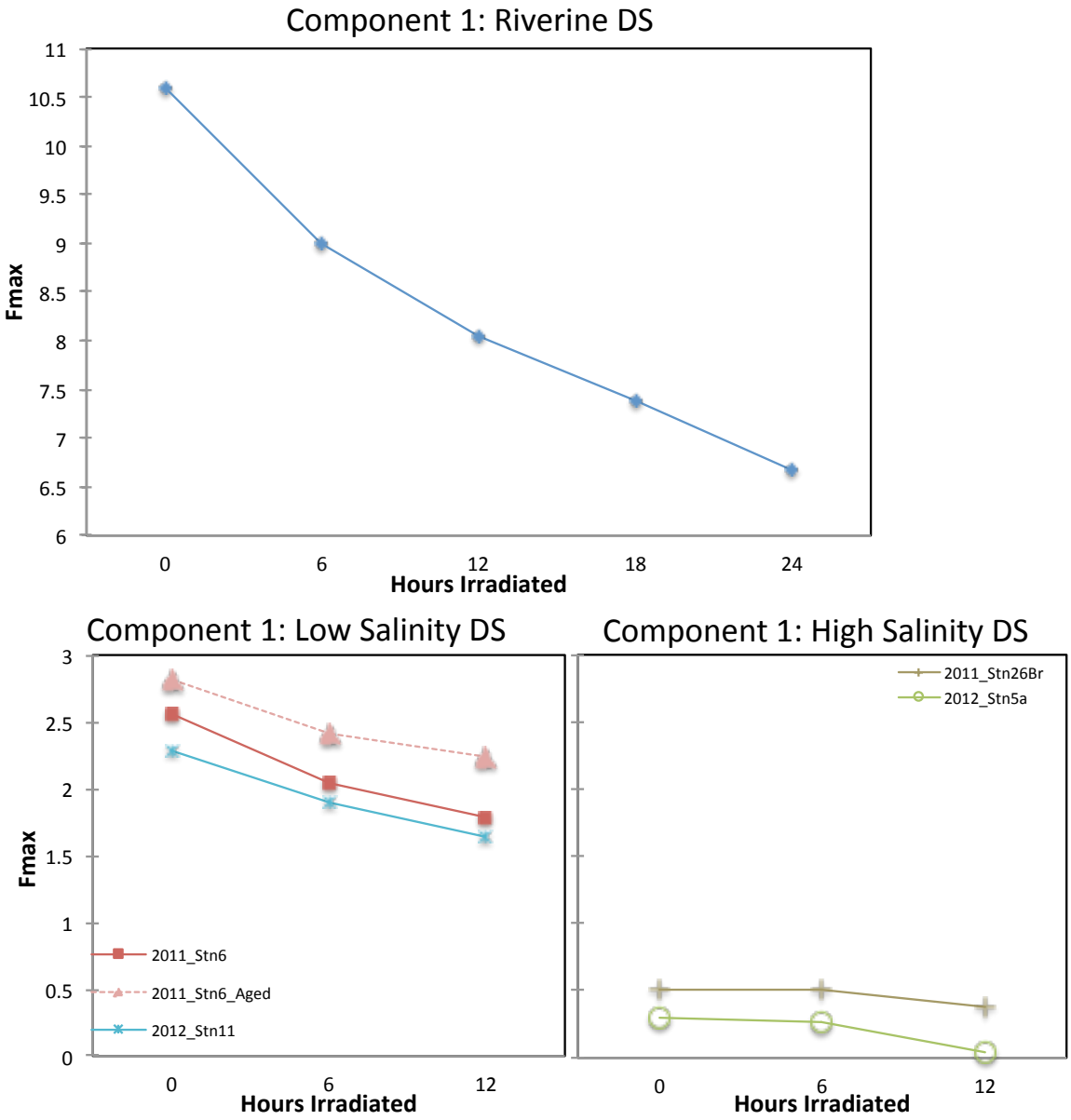

Figure 6: PARAFAC Component 1 as a Function of Irradiation Time

Effects of Irradiation on DOM Source based on Fmax values of PARAFAC Component 1 over the three experimental groups

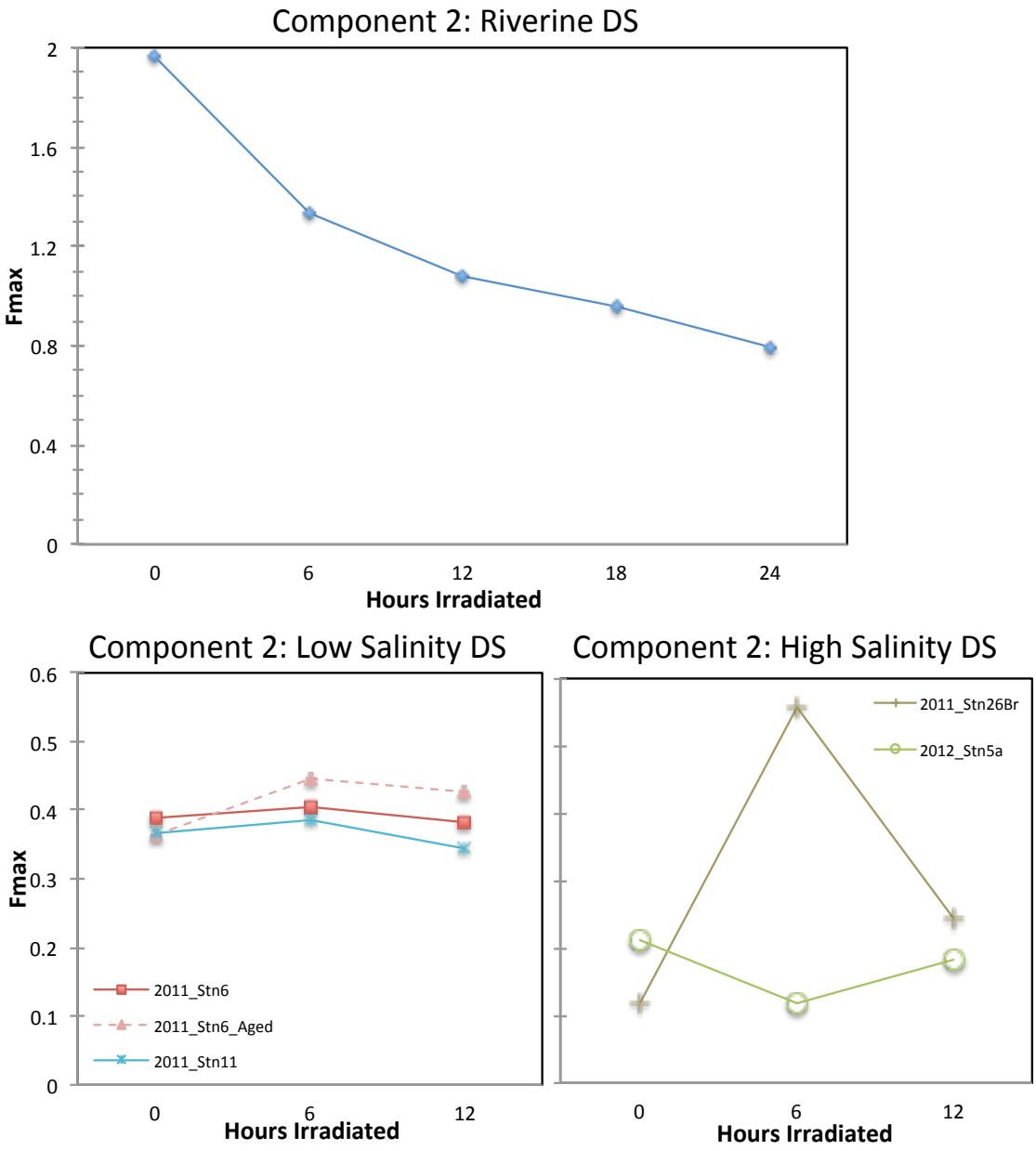

Figure 7: PARAFAC Component 2 as a Function of Irradiation Time

Effects of Irradiation on DOM Source based on Fmax values of PARAFAC Component 2 over the three experimental groups

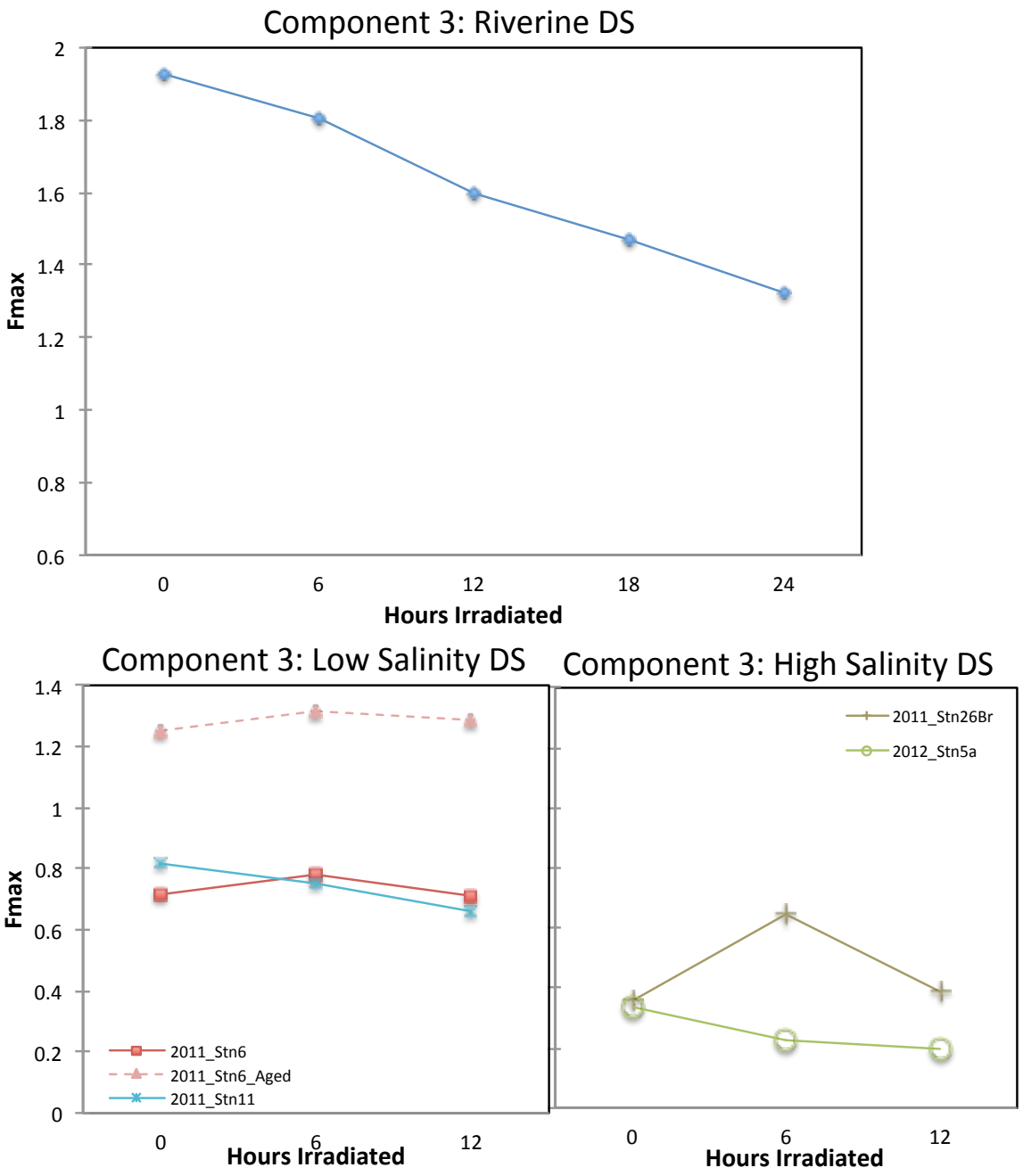

Figure 8: PARAFAC Component 3 as a Function of Irradiation Time

Effects of Irradiation on DOM Source based on Fmax values of PARAFAC Component 3 over the three experimental groups

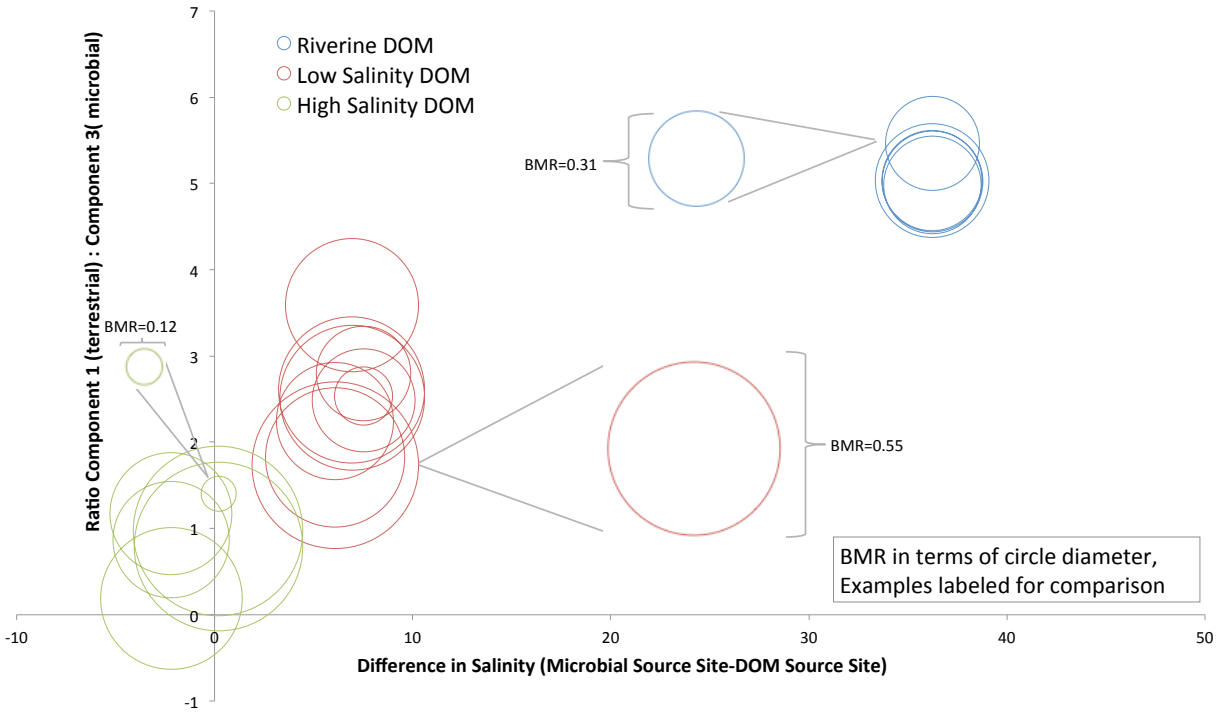

Figure 9: BMR Relative to Differences in Salinity and PARAFAC C1:C3

Bacterial Metabolic Ratios displayed and scaled in terms of the largest value shown (by circle diameter) in experimental grouping by DOM source salinity; X-axis displays salinity difference between Community Source (CS) and DOM Source (DS), Y-axis displays the ratio of DOM components terrestrially derived Component 1 to microbially derived Component 3

A

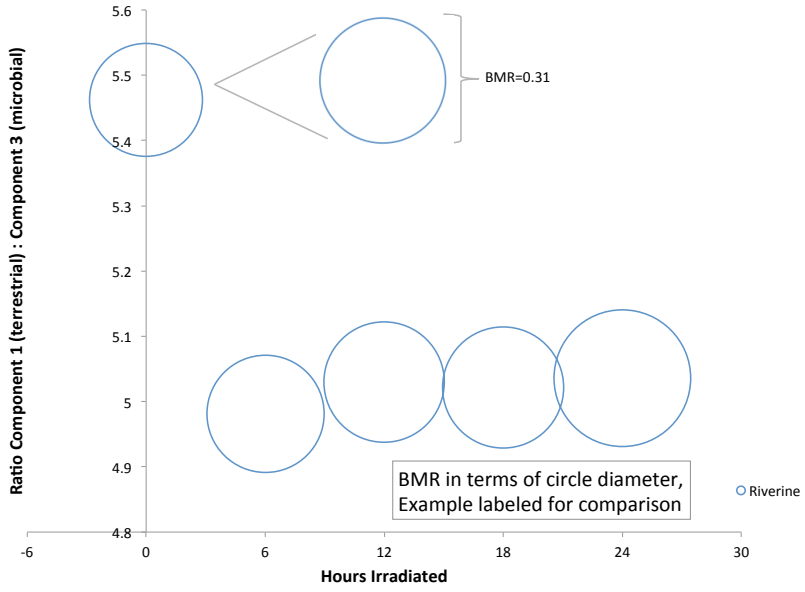

B

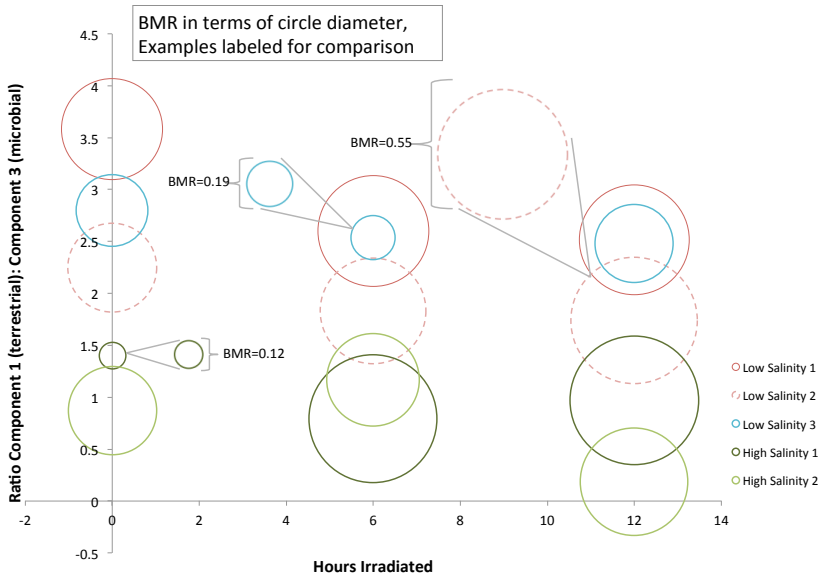

Figure 10: BMR Relative to Irradiations and PARAFAC C1:C3

Bacterial Metabolic Ratios displayed scaled in terms of the largest value (by circle diameter) shown in experimental grouping by DOM source salinity A. =Riverine, B. =Low & High Salinity; X-axis shows hours irradiated, Y-axis shows the ratio of DOM components terrestrially derived Component 1 to microbially derived Component 3

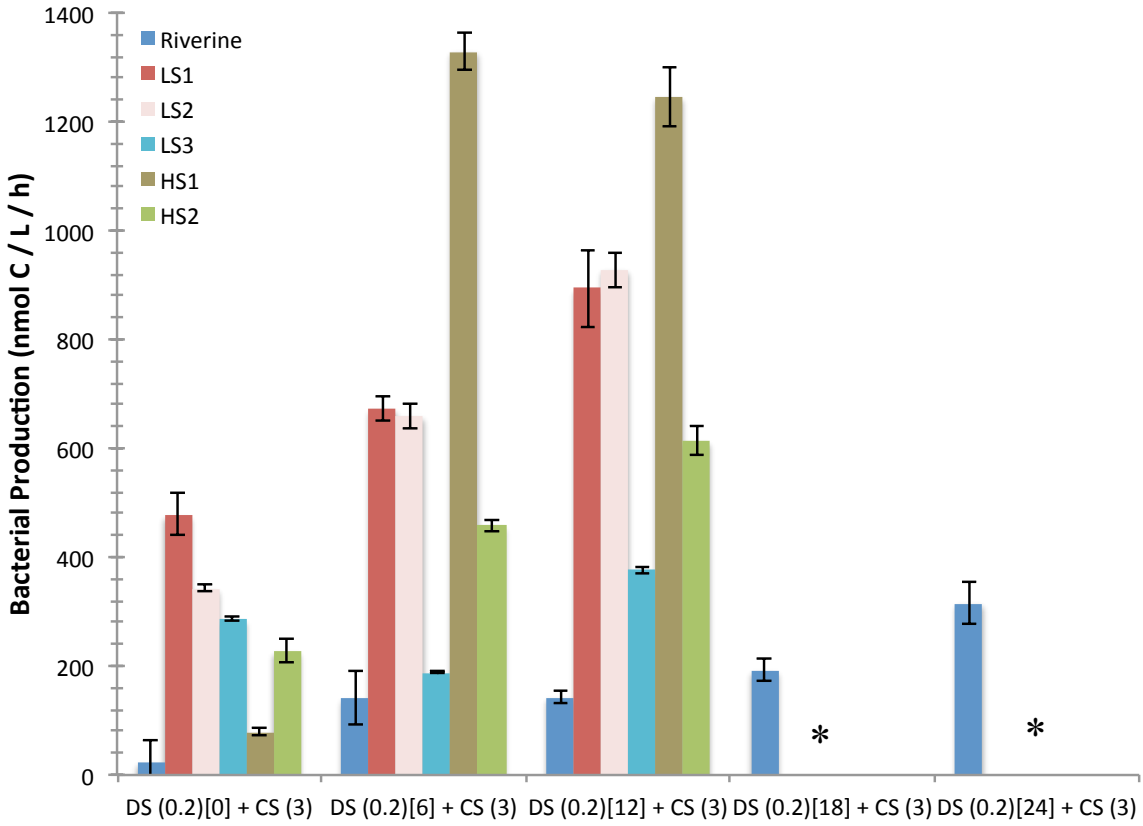

Figure 11: Bacterial Production as a Function of Irradiation Time

*Format for Labels: Sample type (filtration in µm) [irradiation in h], *= No sample collected, DS = DOM Source Water, CS = Microbial Community Source Water*

Appendix A: Sample Processing Diagram

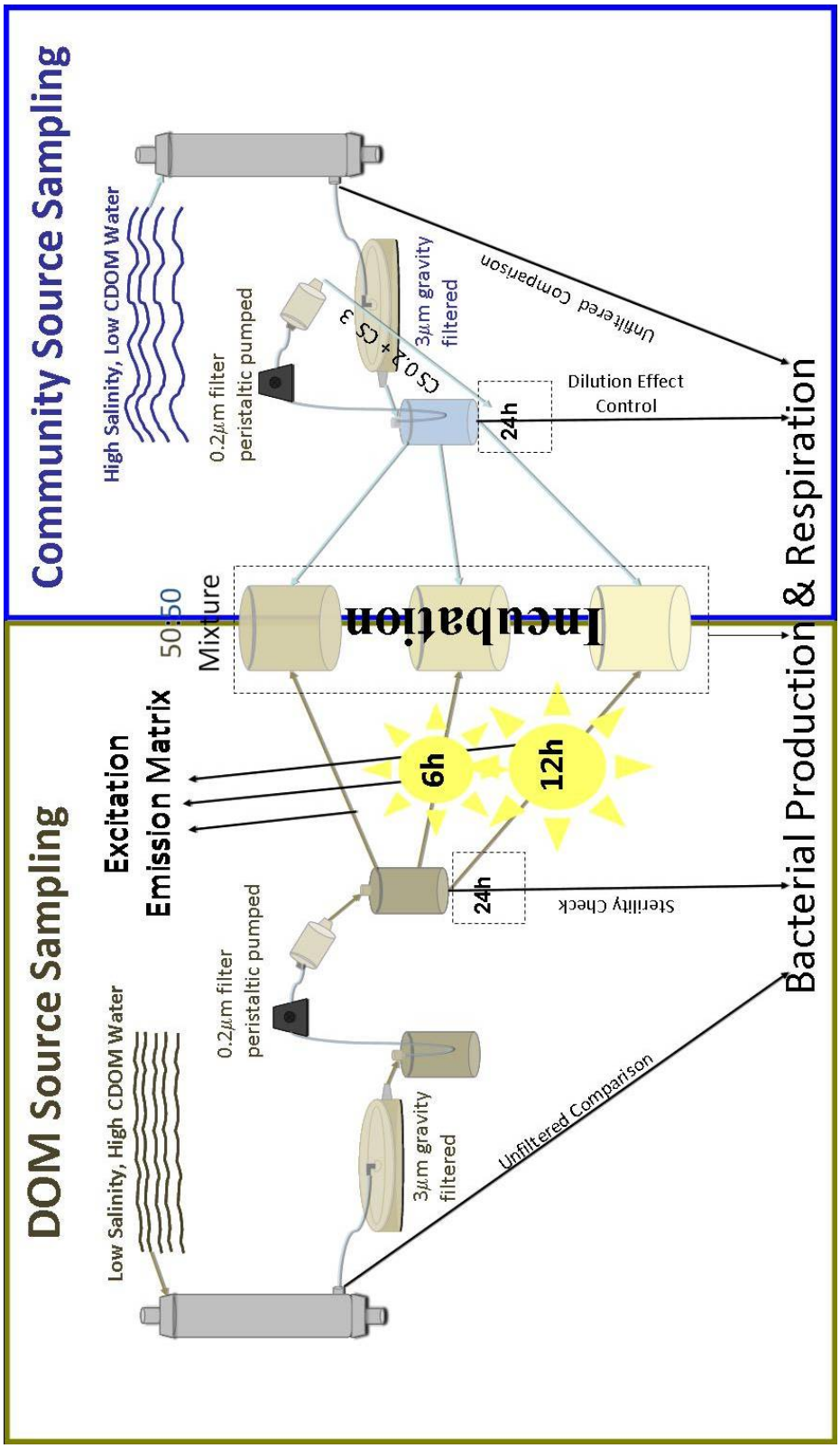

Appendix B: Irradiation Apparatus Diagram

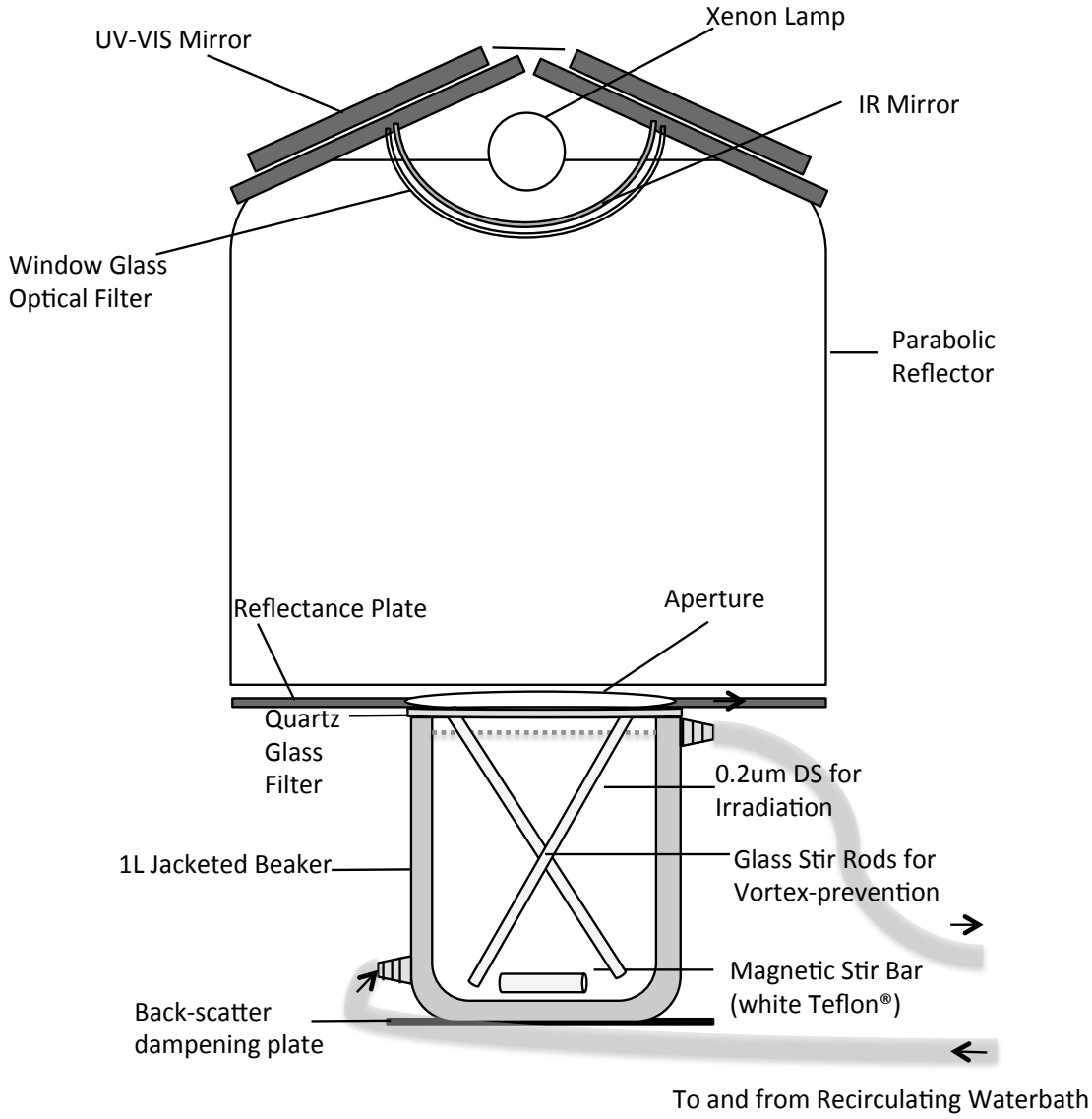

Appendix C: Bacterial Production with Varying Incubation Durations

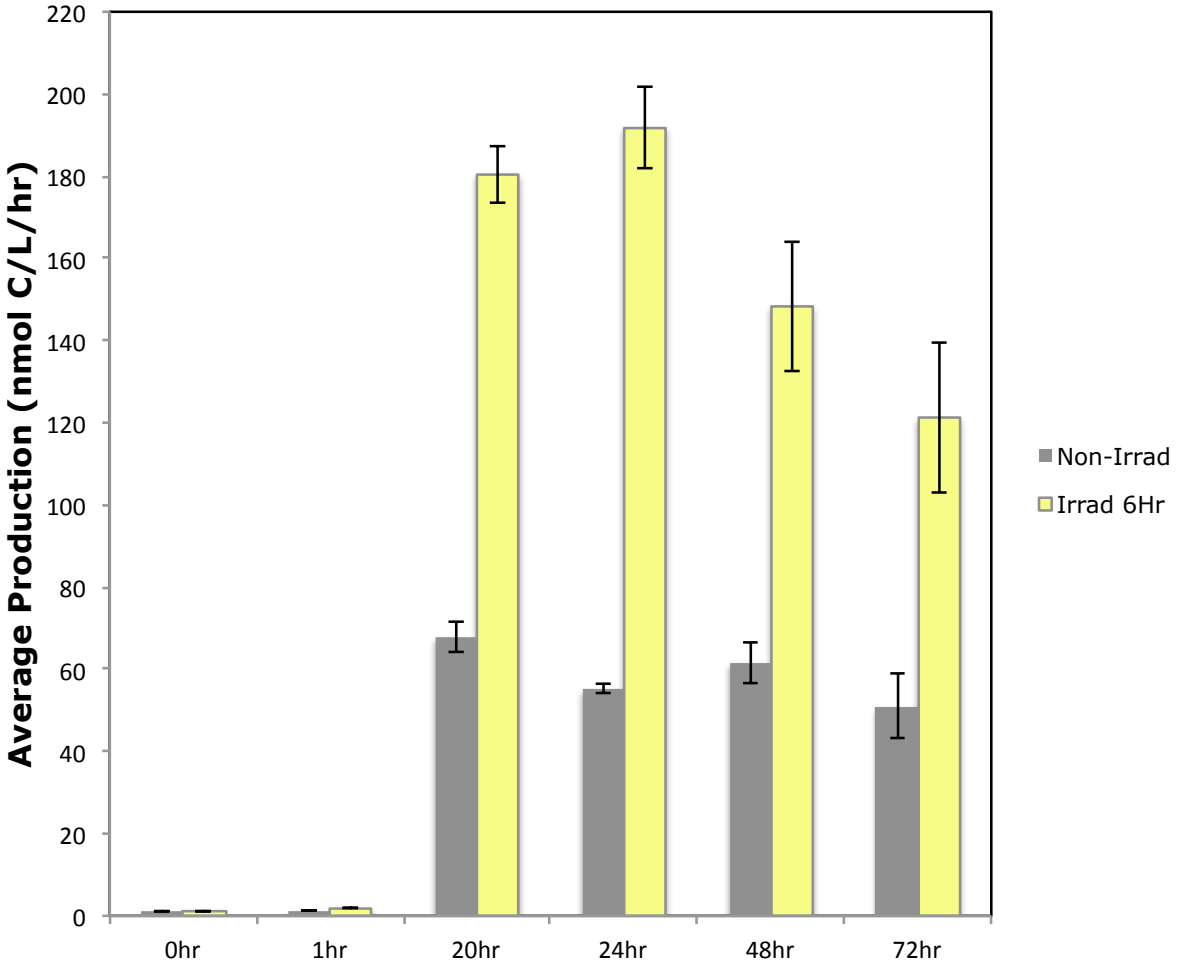

Appendix D: Probe Data Compared to Winkler Data

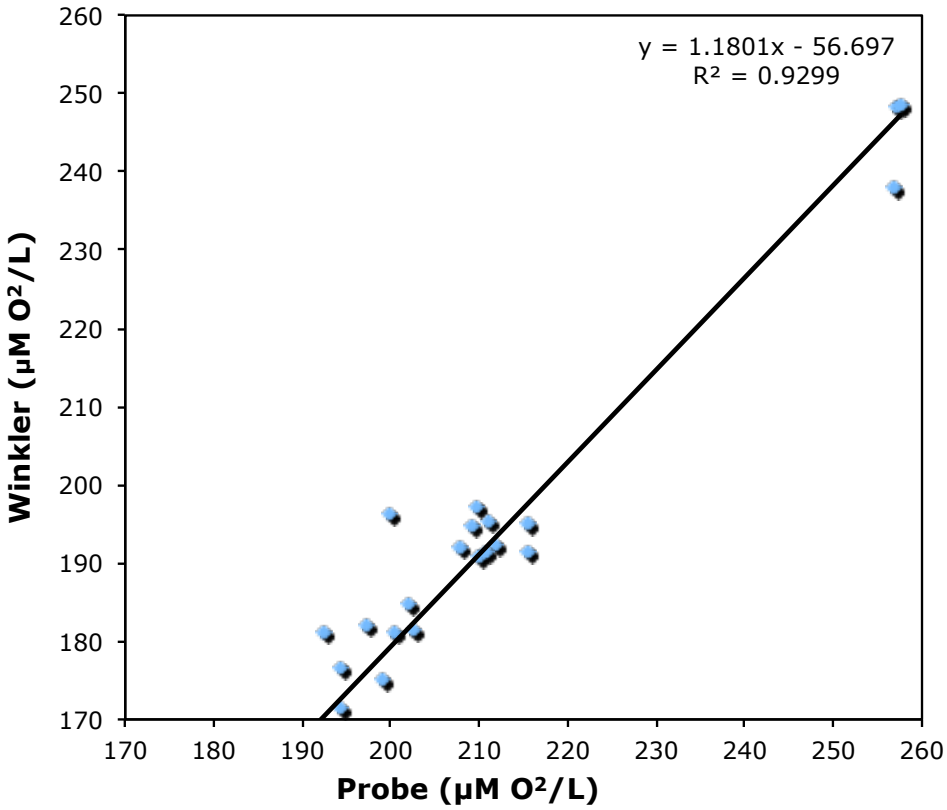

Based on Experiments done by Heather Reader at the University of Georgia. The relationship above was used to correct probe readings so they could be compared to results obtained by Winkler methods.

Appendix E: Varying RQ and Effects on BMR

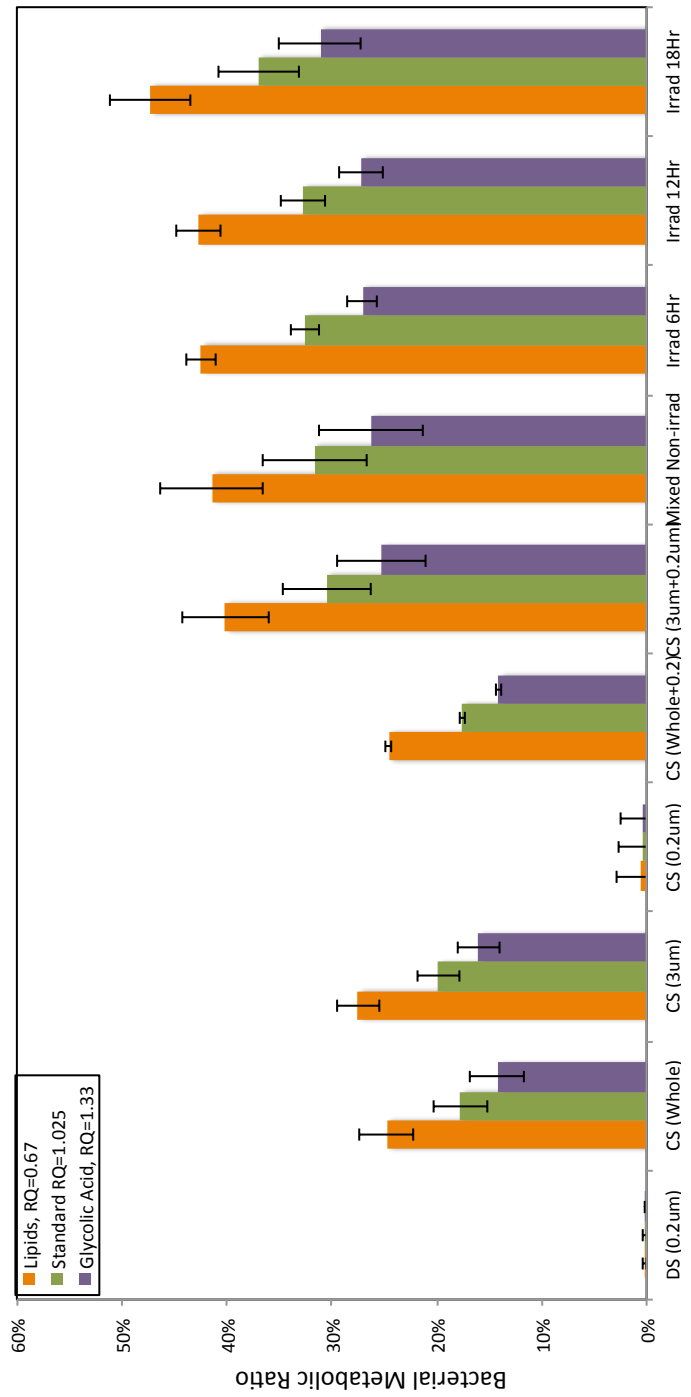

Modeled using 2012 Stn10 (Riverine DOM) with Stn15 marine Microbial community, as these two source waters had the greatest diversity of characteristics

Appendix F: EEMS used for PARAFAC Modeling

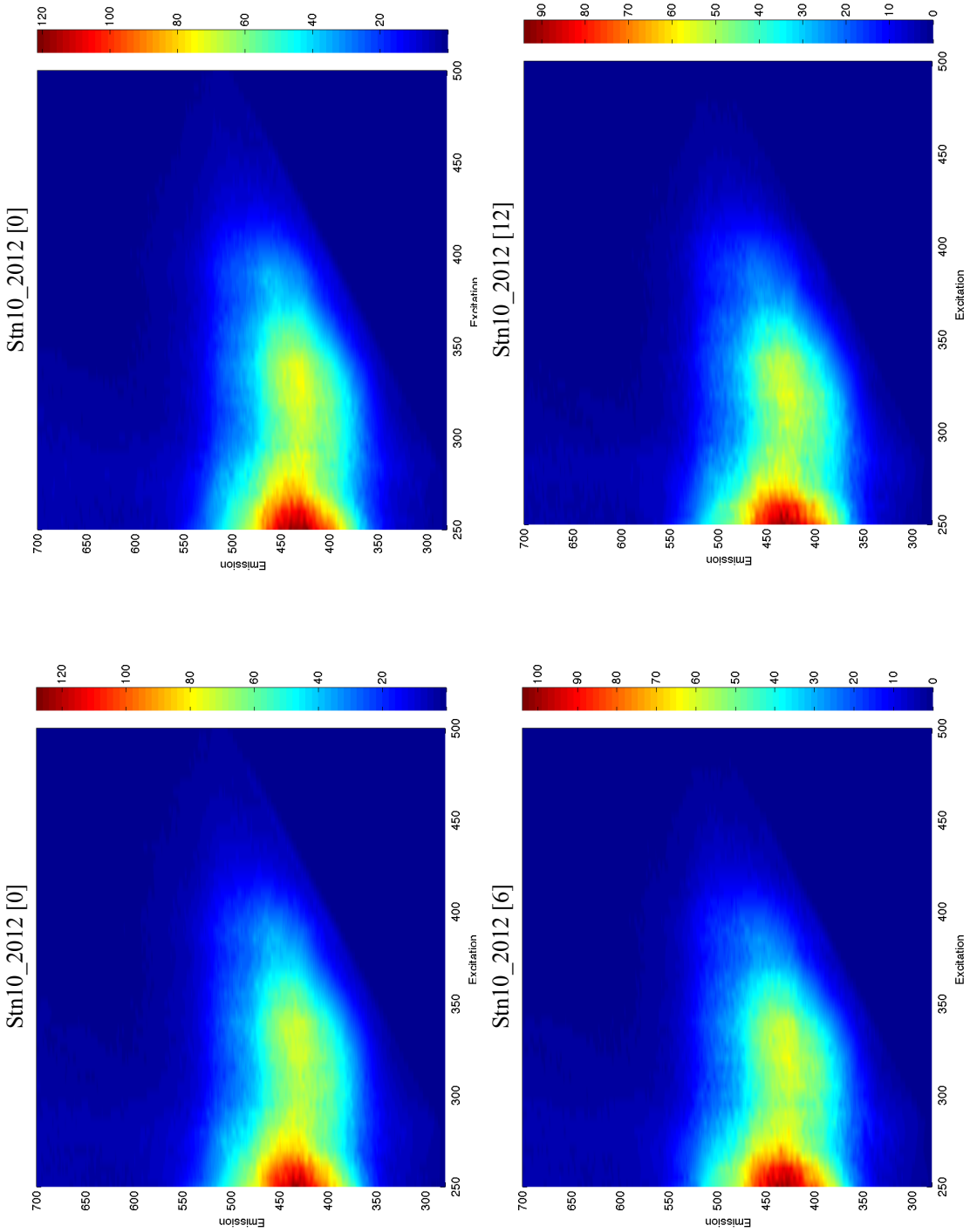

Riverine EEMS [irradiation time], including both duplicates of [0]

Appendix F: EEMS used for PARAFAC Modeling

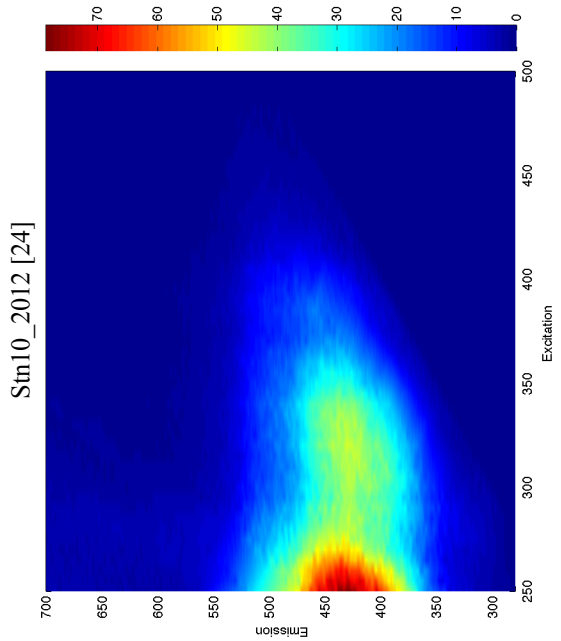

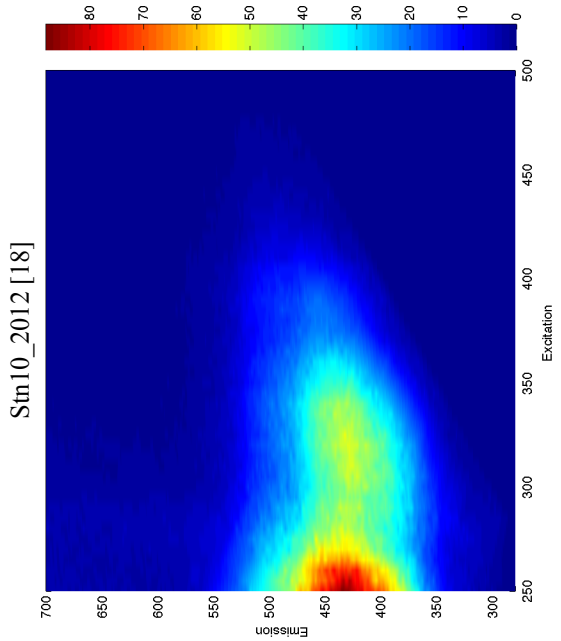

Riverine EEMS [irradiation time], continued from previous page

Appendix F: EEMS used for PARAFAC Modeling

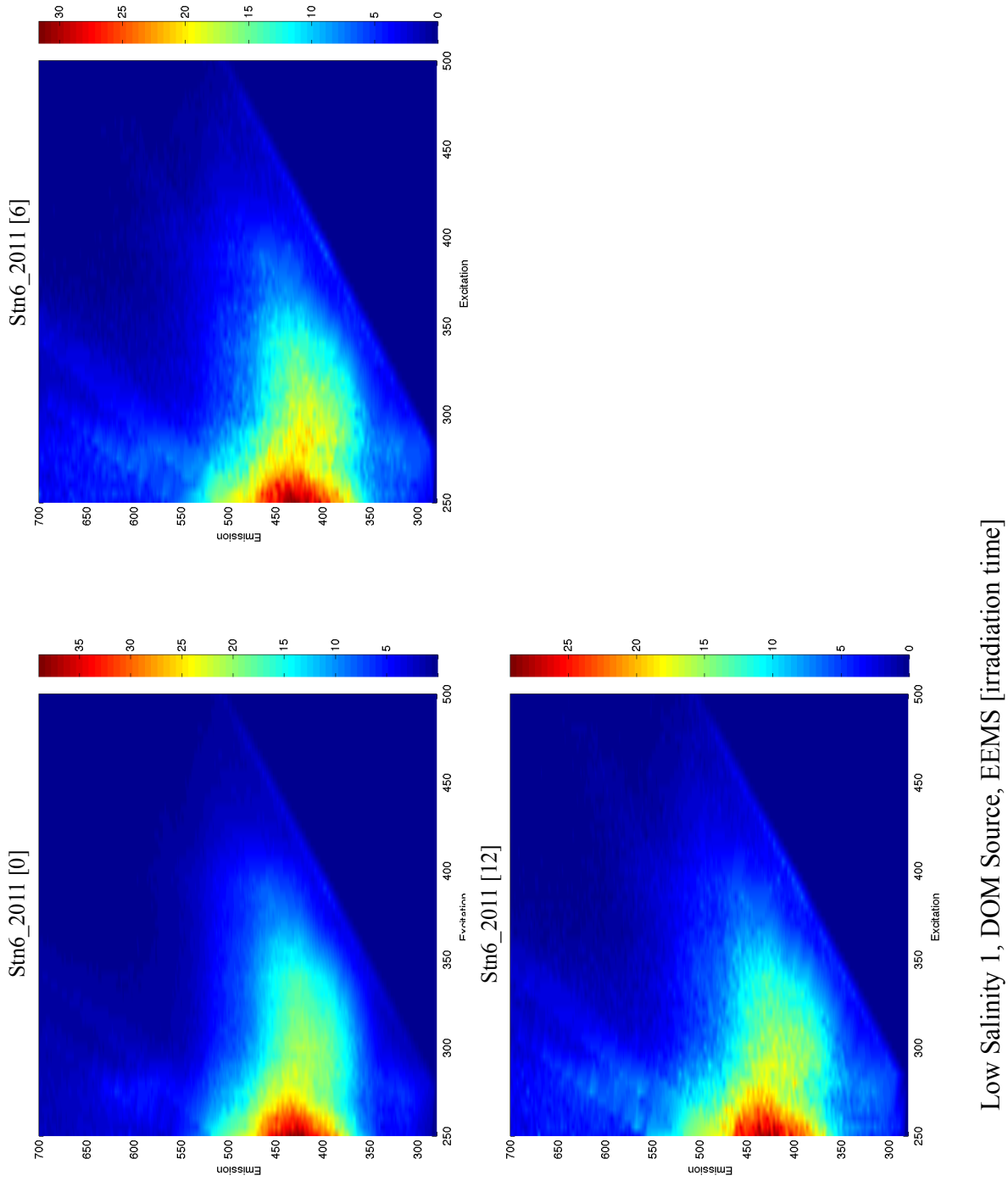

Low Salinity 1, DOM Source, EEMS [irradiation time]

Appendix F: EEMS used for PARAFAC Modeling

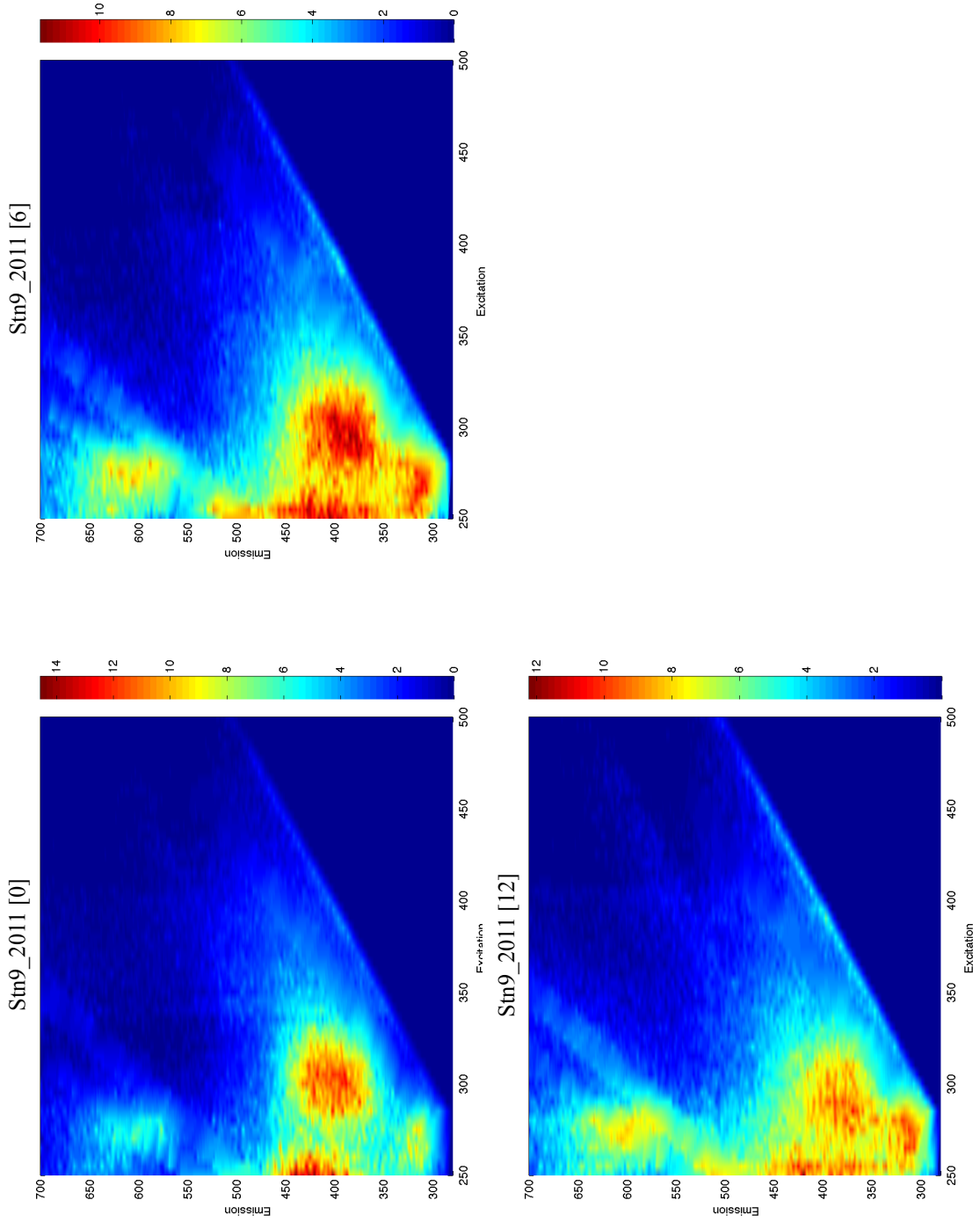

Low Salinity 1, Community Source, EEMS [irradiation time], note: CS irradiations never used in experiments

Appendix F: EEMS used for PARAFAC Modeling

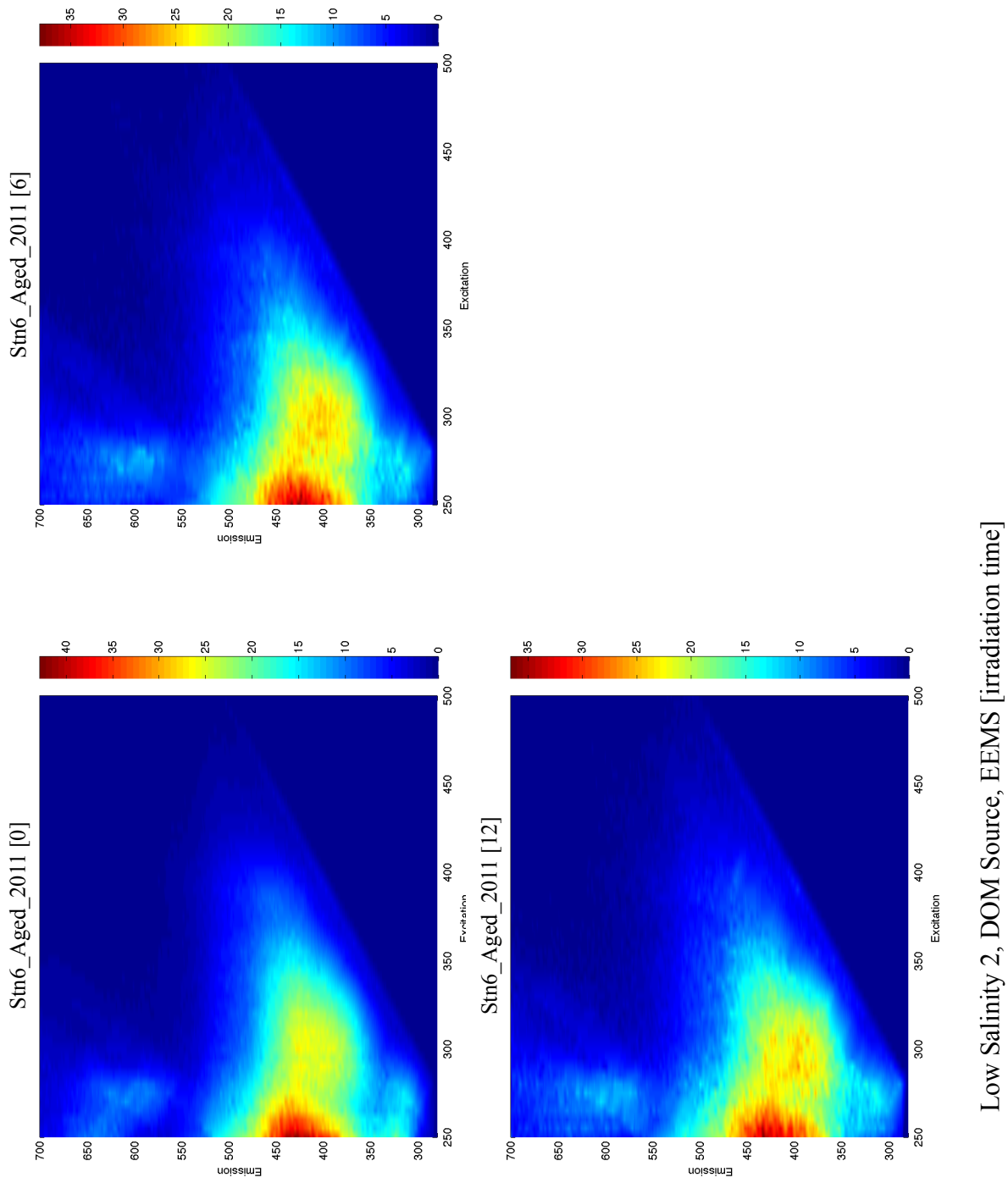

Low Salinity 2, DOM Source, EEMS [irradiation time]

Appendix F: EEMS used for PARAFAC Modeling

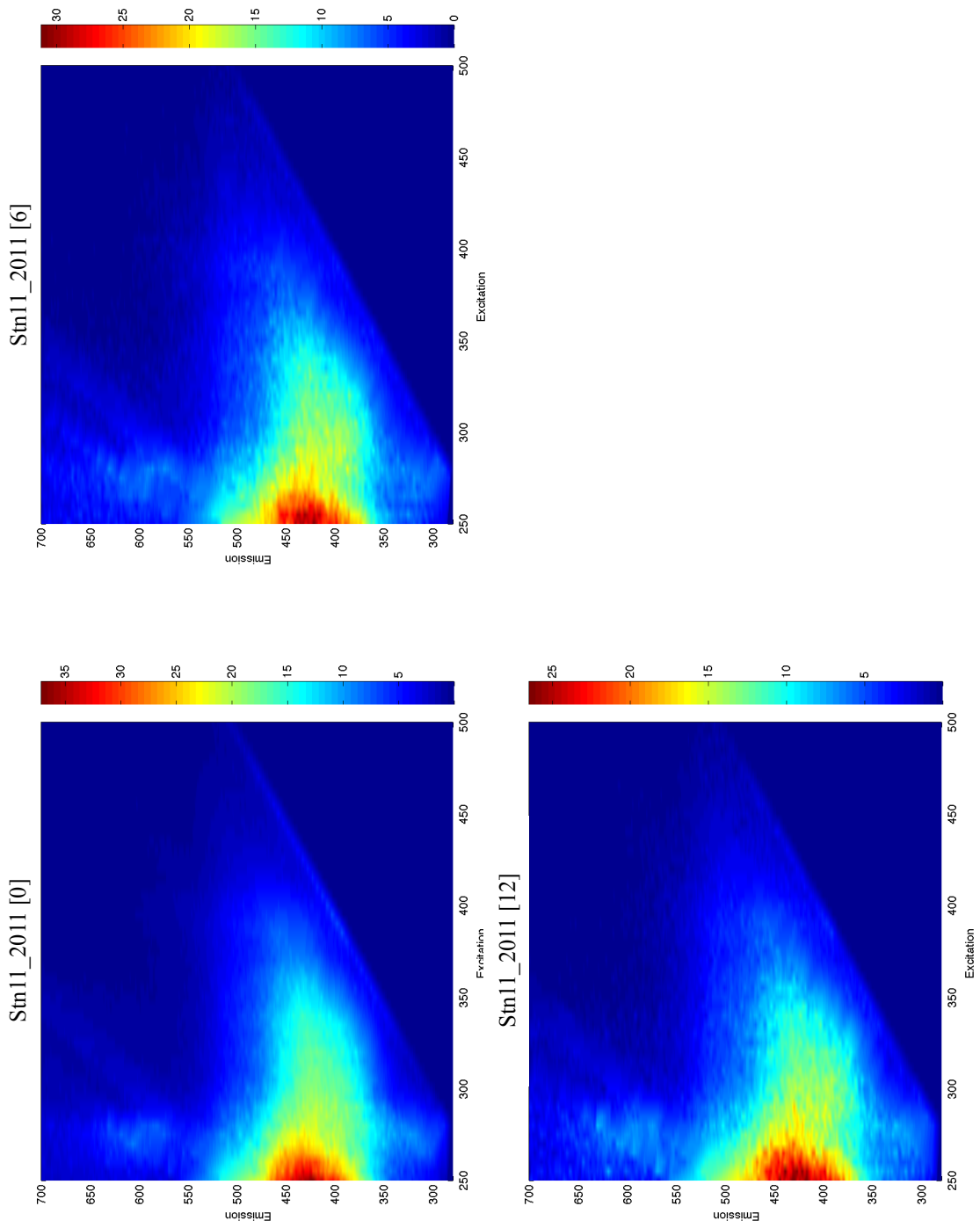

Low Salinity 3, DOM Source, EEMS [irradiation time]

Appendix F: EEMS used for PARAFAC Modeling

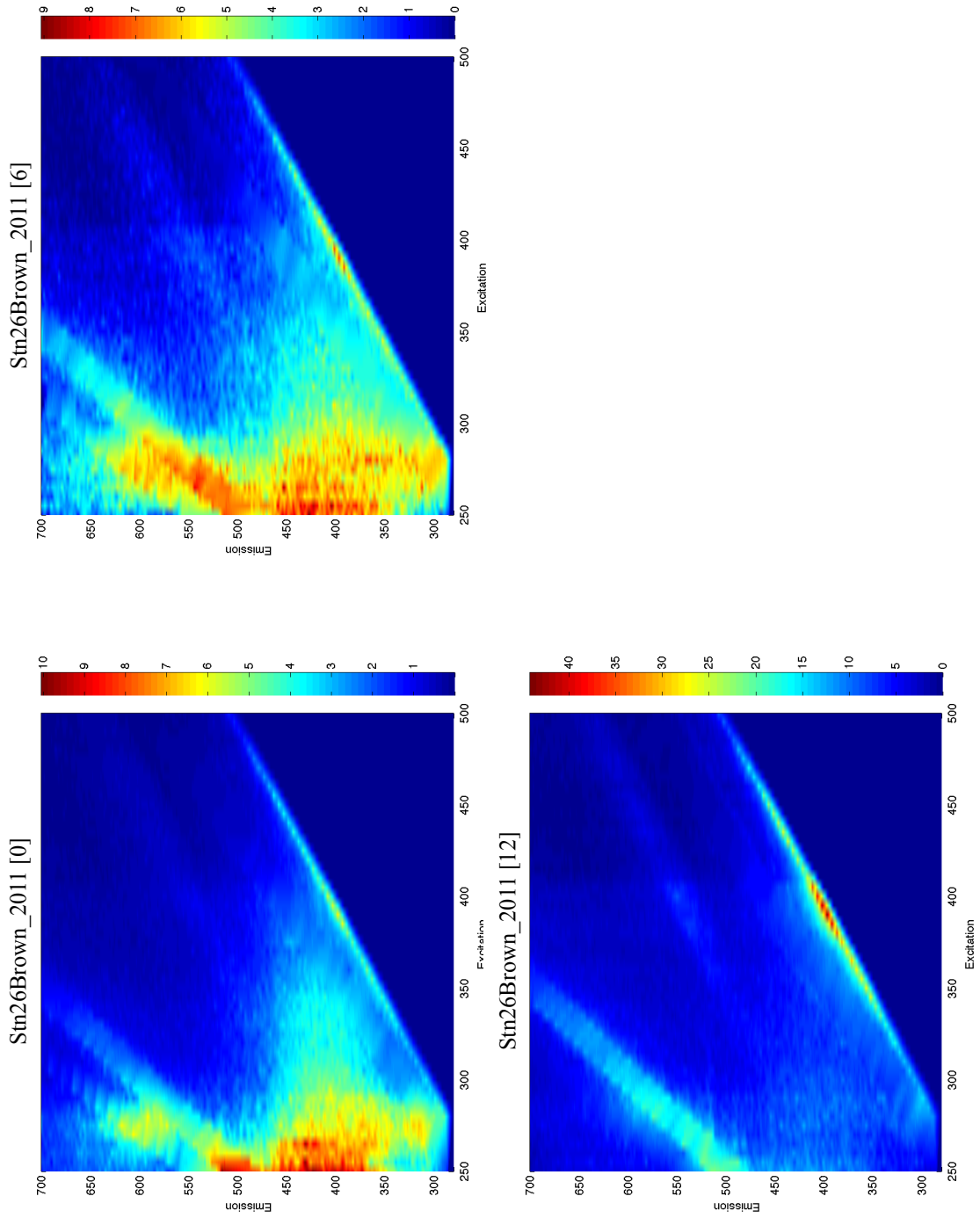

High Salinity 1, DOM Source, EEMS [irradiation time]

Appendix F: EEMS used for PARAFAC Modeling

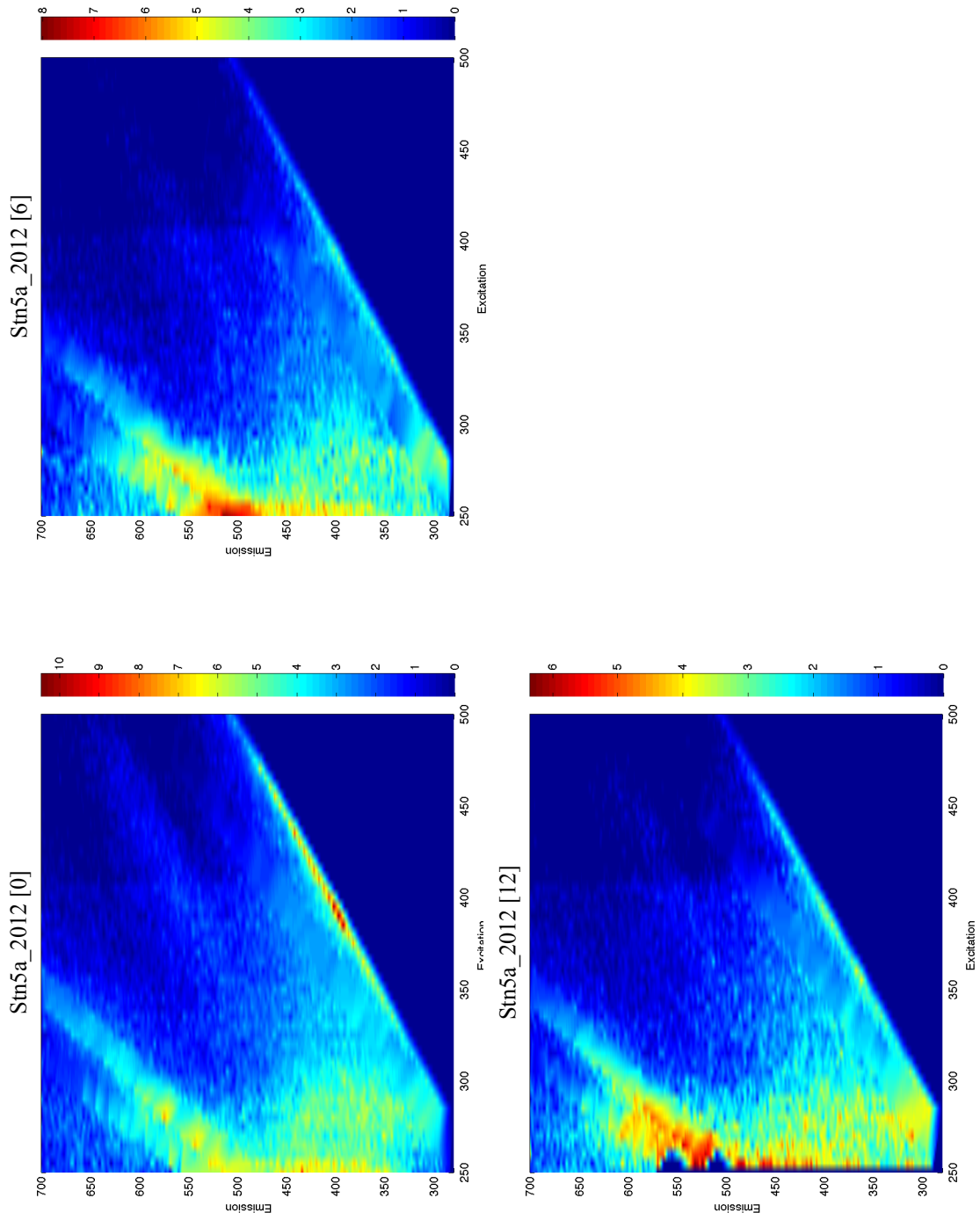

High Salinity 2, DOM Source, EEMS [irradiation time]

Appendix G: EEMS Replicate Assay

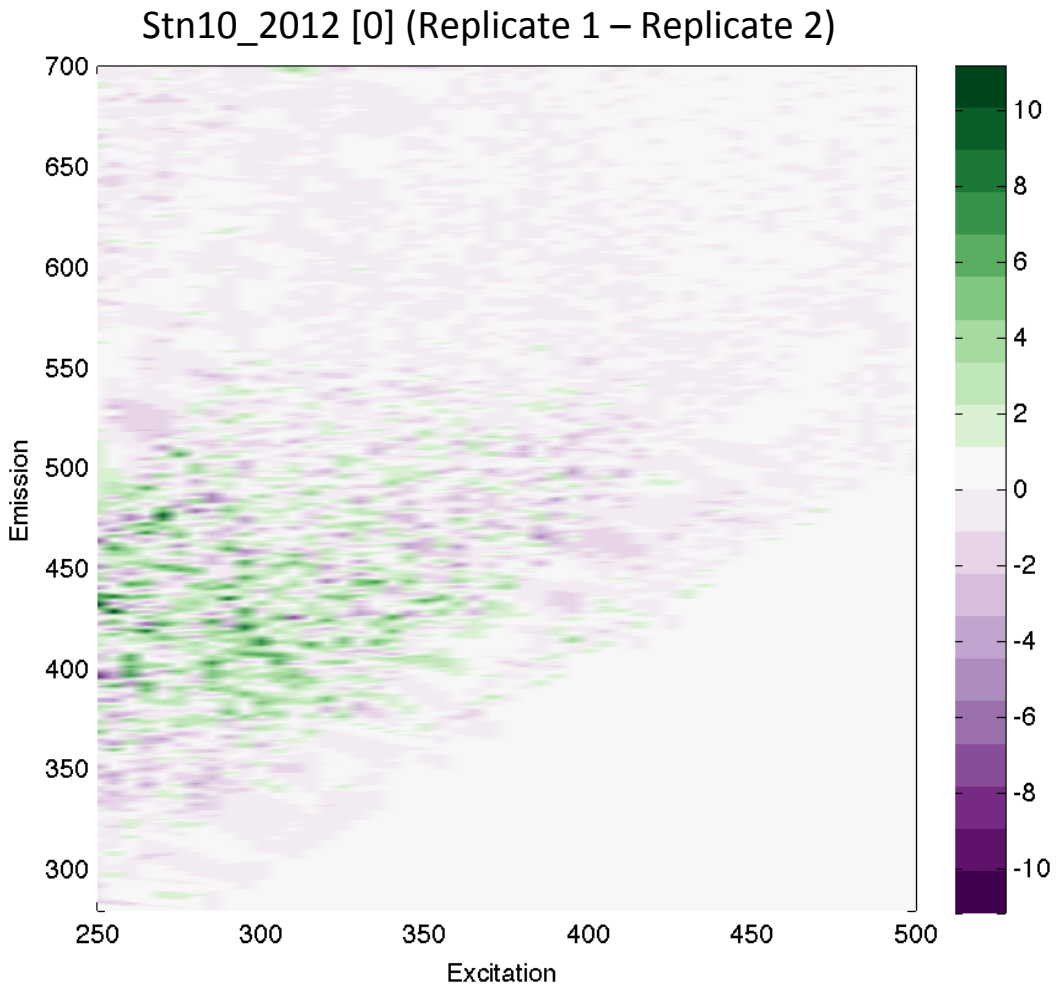

Difference map showing replicability of EEMS: (Fmax Replicate 1- Fmax Replicate 2), visualized using MatLab, color bar represents difference in RU.

Appendix H: EEMS for PARAFAC Components

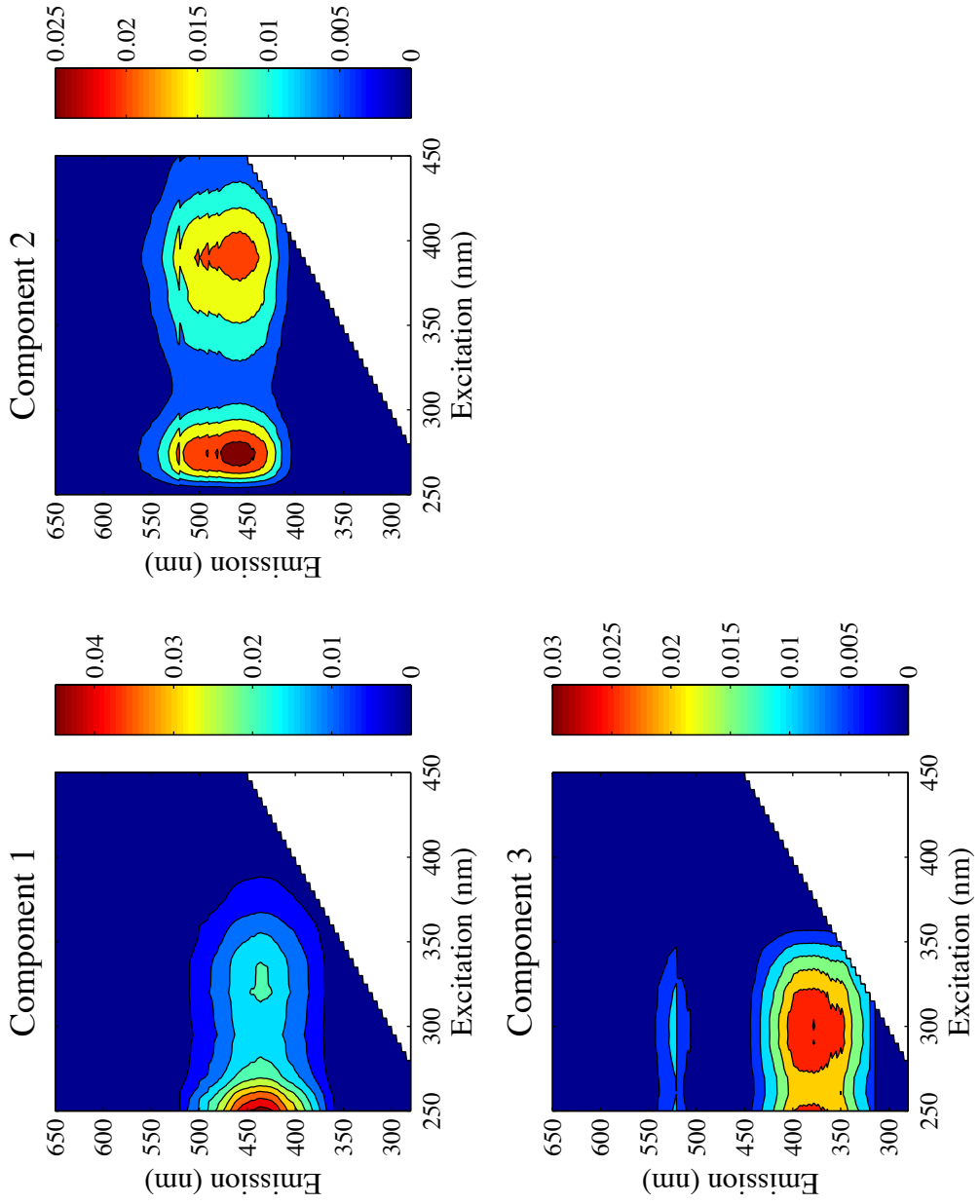

Appendix I: The Physics of a Riverine Plume

Rivers are the active interface between land and the oceans with 87% of the Earth's terrestrial surface included in river basins (Ludwig and Probst 1998). They add huge amounts of dissolved materials to the marine environment each year as well as many tons of soil and rock particles. Rivers also are a major factor in determining global and local salinity. Undeniably rivers are important to the ocean, but what happens when a river enters into the ocean is a far more complicated issue.

Often, features such as plume fronts form where the relatively fresh water reaches an estuary and mixes with the marine environment. This can occur within the lower reaches of the estuary or in the form of a fan that protrudes from the estuary into the coastal ocean. The front around the plume is strongly convergent and turbulent; it is the place where the water from the river begins to homogenize with the oceanic water. Tremendous amounts of energy are released by this mixing. As with any turbulent flow, especially with large transfer of energy, the dynamics are complex, and much is still unknown. However, studies have yielded some information about riverine plume characteristics and oceanic interactions.

Much of what occurs depends on the physical characteristics of the river. Some examples of these factors include discharge rates of both water and sediment, river mouth and continental shelf topography, geographic location, and local climatology and meteorology. Determining which factors are relevant depends on the time scale chosen. For example, tidal effects will be on the order of hours (high vs low) or weeks (spring vs neap). Other physical factors, such as those associated with meteorological processes (winds, waves, mixing) or river discharge (floods, droughts), are on more stochastic time scales and could be manipulated by

anthropogenic forces (watershed development, river or coastal engineering). There are other even longer time scale functions that are seasonal (insolation, temperature, monsoonal), interannual (El Niño/La Niña), and even decadal (climate change, sea levels, precipitation) in occurrence. The cumulative influences of the above factors is likely to result in a non-linear coupling of processes, meaning that there is quite a bit of interconnectivity and feedback (Garvine 1995, Wiseman and Garvine 1995, Yankovsky and Chapman 1997, Dagg et al. 2004).

Often the physical classifications and behavior of plumes depends on the relative magnitude of the convective and Coriolis force accelerations, wind and benthic induced stress, and baroclinic pressure gradients/buoyancy (Garvine 1995). Convective forces would come into play when there was a large temperature difference between the riverine and marine waters. As the Coriolis force is related to latitude, those rivers at higher latitude would be much more affected than those closer to the equator. The other factors are more difficult to generalize and often some research will neglect them with an assumption of applicability within certain time limits.

Yankovsky and Chapman suggest two major classifications of plumes; bottom-advected and surface-advected(Yankovsky and Chapman 1997). Bottom-advected plumes are controlled by advection in the bottom boundary layer, where the buoyant flow spans the entire shelf area with the frontal zone appearing at the shelf-break. These plumes range offshore more than 100 km and have a maximum depth of approximately 200 m. Surface-advected plumes remain on top of the shelf water, forming a thin layer with the denser marine water beneath and little to no contact with the bottom, except perhaps close to shore. This type of plume ranges from 10-15 km offshore with a depth of no more than 10m. For both Yankovsky and Chapman models, tides and wind forcing were not included. Their models focus primarily on buoyancy and density by

incorporating the Burger number as a measure of buoyancy, and the Rossby number as a measure of nonlinear advection or rate of inflow through the river mouth. The other inputs to the model are the depth and bottom slope of the isobath between plume water and marine water and horizontal seaward expansion of the plume.

Wiseman and Garvine used a model for creation and maintenance of a buoyant plume based on shorter timescales, and what they considered near-field regions close to the mouth of the river. Therefore it focuses on tides and wind forcing, and combines that information with potential rotational effects of mixing via the Kelvin number (K) (using width of discharge and Rossby radius). The Rossby radius was computed using densities of plume versus coastal water, Coriolis, plume depth, and acceleration due to gravity (Wiseman and Garvine 1995). They determined that plumes with a small K would allow for deflection of the plumes along with the coastal currents, and would not be greatly affected by the Coriolis force, besides a transient anti-cyclonic eddy at the mouth. Flows with a larger K value will often create a large freshwater bulge in anti-cyclonic flow corresponding to the strength of the Coriolis force in the region. However a strong wind forcing and coastal currents might still be able to deflect the plume along the coast depending on the plume depth (Wiseman and Garvine 1995, Isobe 2005). The eventual fate of most plumes is in geostrophic flow within the coastal Kelvin waves (Wiseman and Garvine 1995, Nash and Moum 2005). However, a notable exception is the Amazon River, which is unique due to the immense flow rate, resulting depth of plume, and location/low Coriolis forcing (Geyer et al. 1991, Wiseman and Garvine 1995).

Kourafalou and colleagues used models to define two main types of plumes: supercritical and subcritical(Kourafalou et al. 1996). These divisions are not comparable to those used by

Yankovsky and Chapman, and focus on discharge and shear; comparing the freshwater bulge formation with the coastal current strength, in terms of Richardson number (the ratio of potential to kinetic energy) (Kourafalou et al. 1996, Yankovsky and Chapman 1997). A supercritical plume is created when the discharge rate and shear velocity is greater than 1, meaning that the anti-cyclonic bulge is greater than the width of the coastal current. The reverse is true for a subcritical plume. This is similar to that discussed by Wiseman and Garvine (Wiseman and Garvine 1995). However, the Kourafalou et al. models utilized a "line source" definition as well as the standard "point source" definition of rivers, which created the potential for more off-shore transport. This modeling did take in account some boundary conditions, though these were less descriptive than for Yankovsky and Chapman, but many other inputs were utilized (Yankovsky and Chapman 1997). The results from this extensive modeling approach are not completely straightforward, although there are several salient points. Rotation and nonlinear forcing were more important when there was a lack of wind stress. Supercritical plumes not only create large fresh-water bulges, but also cause coastal current meandering where the current comes into contact with the bulge. This meandering is a result of baroclinic instability created by the stratification of the plume and marine water. Subcritical plumes have greater mixing or shallow depths that will not allow for maintenance of the stratification. The speed of winds can affect plume mixing and buoyancy-driven flow. Light winds (less than 5m/s) will not noticeably change a developed plume, whereas a strong wind (5-10m/s) has the potential to fully reverse the buoyancy-driven flow, depending on the strength of the plume. Maintained stratification of a plume region can enhance offshore Ekman transport during high river flow with up-welling favorable winds (Kourafalou et al. 1996).

Despite being highly idealized, numerical modeling has helped elucidate some important

dynamics between a riverine plume and the marine system. However, given the nature of turbulent flow and the transient forces involved, it is highly unlikely a plume is in steady state, which is an assumption of most models. Plumes in nature are rarely unforced and the time scale observed will determine which forces are the most relevant (Garvine 1995). Rivers undeniably deliver material to the oceans, but these materials are not necessarily immediately available, as they can be entrained within a plume front (Ludwig and Probst 1998). The mixing and transport of riverine plumes and the physical parameters of rivers cannot be ignored when considering coastal environments and the marine system as a whole.